(19) Europäisches Patentamt
European Patent Office
Office européen des brevets

(11) EP 1 469 548 A1

(12) EUROPEAN PATENT APPLICATION

(43) Date of publication:
20.10.2004 Bulletin 2004/43

(51) Int Cl.[7]: **H01P 1/213**

(21) Application number: **03425240.3**

(22) Date of filing: **18.04.2003**

(84) Designated Contracting States:
AT BE BG CH CY CZ DE DK EE ES FI FR GB GR HU IE IT LI LU MC NL PT RO SE SI SK TR
Designated Extension States:
AL LT LV MK

(71) Applicant: **Siemens Mobile Communications S.p.A.**
20126 Milano (IT)

(72) Inventors:
- **Bonato, Paolo**
  20156 Milano (IT)
- **Morgia, Fabio**
  20125 Milano (IT)
- **Gaiani, Danilo**
  20052 Monza (IT)
- **D'Orazio, Antonella, Prof.**
  70121 Bari (IT)
- **Fera, Pasquale**
  70121 Bari (IT)

(74) Representative: **Giustini, Delio**
Siemens Mobile Communications S.p.A,
Palazzo Gorky
Via Monfalcone, 1
20092 Cinisello Balsamo (IT)

(54) Microwave duplexer comprising dielectric filters, a T-junction, two coaxial ports and one waveguide port

(57) Duplexer filter is constituted by a metallized alumina substrate (11) interposed between a robust metallic base (14) and a metallic hollow body (17) milled as a short waveguide tract fixed to the metallic base. The free end of the hollow body (17) is connected to an R140 mechanical waveguide connected to the antenna feeder at the other end. The metallized layout includes two dielectric resonant cavities (CVL, CVH) at the two sides of a central unmetallized gap (GP) on the upper face of the alumina. Each dielectric cavity terminates with a tapered transition (TPL, TPH) towards a microstrip conveying either the transmission or reception signal towards either the high or low bandpass dielectric filter (BPL, BPH) built up on the cavity. The metallic hollow body (17) includes a terminal tract with reduced section (MC-T) whose rectangular opening is faced to the central unmetallized gap (GP) between the two dielectric filters. The walls of the hollow body (17) delimiting the central opening are soldered (by brazing) to the metallic layout delimiting the central unmetallized gap, in order to keep the two dielectric cavities of the filters and the metallic cavity of the hollow body contiguous to each other. The central part of this structure constitutes an extremely compact T-junction including two identical transitions between dielectric and mechanical waveguide, and vice versa, without the need of separate excitation means as probes or irises. The dielectric cavities of the two filters include metallized through holes acting as inductive posts for shaping the separate bandpass responses in a no-tuning way. In a preferred embodiment of the duplexer the central unmetallized gap (GP) of the alumina substrate projects itself outside the original rectangular profile for optimising the design of the T-junction. The enlarged gap is surrounded by a metallized frame (12, 13) for shielding and simplifying the sealing (by brazing) of the space at the two short sides of the gap (fig.10).

EXPLODED VIEW OF THE DUPLEXER FILTER

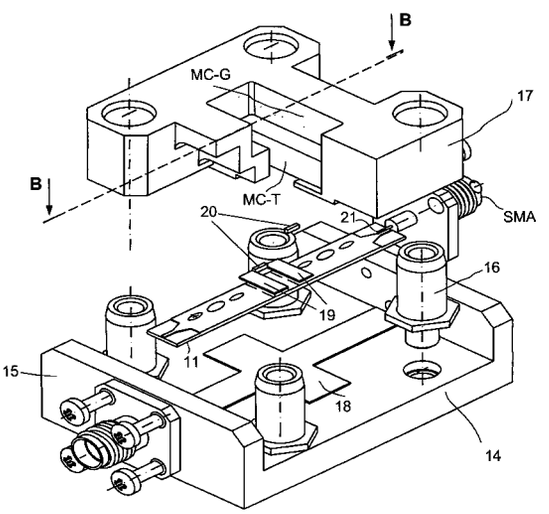

FIG.10

EP 1 469 548 A1

Description

FIELD OF THE INVENTION

[0001] The present invention is referred to the field of the duplexer filters and more precisely to a microwave duplexer integrating dielectric and hollow mechanical waveguides into a compact T-junction.

BACKGROUND ART

[0002] In the known front-end designs for transmitting and receiving communication equipments exploiting a single antenna, the separation of the transmit power from the circuitry of the receiver is fundamental. Without such separation many problems are encountered, for example the transmit signal causing feedback into the system and reducing its sensitivity, or the transmit power saturating the receiver components possibly to the point of destroying them. High power into a sensitive low noise amplifier can be disastrous. Duplexers are well known countermeasures used in communication systems based on Frequency Division Duplexing (FDD) with received and transmitted signals simultaneously collected by the same antenna. Canonical functional schemes of duplexers are reported in **figures 1** and **2** referred to the use of circulators or hybrid T-junctions, respectively.

[0003] **Fig.1** shows the structure of a front-end including a TRANSMISTTER, a RECEIVER, a duplexer DPX, and an antenna (not visible). The duplexer DPX is represented as a three ports circuit having a first port 1' for the input of an RF transmitted signal TX, a second port 2' to be coupled to an antenna, and a third port 3' for outputting a received signal RX. The duplexer DPX includes a first bandpass filter BP1, a ferrite circulator CIR, and a second bandpass filter BP2 having a central frequency higher than BP1. The ferrite circulator CIR has three ports 1, 2, and 3 whose directional properties are well known from the canonical books in microwave filter design [**1**], [**2**], and [**3**] indicated in the References at the end of the disclosure. Filter BP1 is placed between the input 1' of DPX and the port 1 of the circulator CIR; filter BP2 is placed between port 3 of CIR and the output 3' of the duplexer DPX; while the input-output port 2 of the duplexer CIR also coincides with the port 2' of DPX connected to the antenna. Thanks to the directional property of the ferrite circulator CIR, the TX signal at port 1 reaches the port 2 but not the port 3, and the RX signal at the port 2 reaches the port 3 but not the port 1; that is, the transmission signal TX is separated from the receiver RX input. On the antenna connection to the port 2' the TX frequency band is intrinsically separated from the RX frequency band by the FDD design. **Fig.2** shows a duplexer filter DPX which differs from the one of **Fig. 1** only by the replacement of the circulator CIR with a hybrid T-junction, also disclosed in the same cited references. The difference from a circulator and a hybrid T-junction is that the first, being a non-reciprocal and non-dissipative ferrite device, is simultaneously matched at the three ports, while the second is a reciprocal device not simultaneously matched at the three ports.

[0004] Popular embodiments of the duplexers of the **figures 1** and **2** suitable to be used in the microwave frequencies have a simple hollow mechanical waveguide structure including some discontinuities, such as iris diaphragms or small cylindrical rods (the so-called "inductive posts"), in order to shape the frequency response of the resonant cavities with the required selectivity. These filters have great robustness and reliability, low insertion-loss, and sharp cut-off in the rejected bands because of their high-Q values, but generally require an accurate manual tuning due to the mechanical tolerances. Besides, a duplexer realized in an hollow mechanical waveguide is cumbersome, just as the opposite of the current trend towards the miniaturisation of the telecommunication equipments especially in the field of cellular telephony. To solve this problem a drastic reduction of the dimensions has been obtained by dielectric filters exploiting dielectric materials with relative permittivity ε_r >1. The achieved dimensional reduction is proportional to $\sqrt{\varepsilon_r}$. Dielectric filters include dielectric resonators (DR) obtained by deposition of thin metallic layers on the surfaces of dielectric substrates, e.g. alumina. Considering that for the alumina ε_r =9.8, the obtained reduction is in the order of 3.13 times. A particular case of highly miniaturised and efficient dielectric filters are based on Surface Acoustic Waves (SAW). The higher precision of the manufacturing process of the dielectric filters, in comparison with the tolerances of the mechanical waveguides, makes the tuning operations often unnecessaries.

[0005] An example of duplexer using two dielectric bandpass filters connected to a microstrip T-junction is disclosed in the paper of **Ref.[4]**. The duplexer includes RX and TX filters designed as three-stage Tchebyscheff bandpass. Each stage is embodied with a high-permittivity ceramics dielectric resonator, with: ε_r =24, Q = 2600; the three resonators are aligned along the central longitudinal axis of a rectangular metallic cavity filled up with a dielectric resin with lower permittivity. Two microstrip lines are inserted into the metallic cavity to weakly couple with the three-stage resonator at its both ends. The bottom surface of the rectangular cavity is partially grooved under the outer-side ends of dielectric roads to fix the microstrip substrates. The T-junction is a microstrip layout shaped as a T, whose horizontal branches are individually connected to the microstrip lines of the RX and TX filters, respectively, and the right-angle branch shall be connected to the antenna (not visible). Ideally, the electrical length of the two aligned branches should be determined as that in the TX band the input impedance of the RX filter at the junction-point is infinite, and vice versa. The advantages of dielectric duplexers are nevertheless not plenty appreciable when an hollow

mechanical waveguide is used for the connection to a remote antenna; this is due to the difficulty of designing suitable transitions for coupling RF signals between the dielectric filters and the mechanical waveguide. In fact, other than the electromagnetic coupling through the transition, even the mechanical coupling has to be considered. From a mechanical point of view the difficulties arise from the different physical properties of the two bodies; for example, mechanical waveguides are hard and stiff while alumina substrates are hard but fragile. Alumina does not bear excessive strengths in the contacting zone with the metallic waveguide, because might be easily broken up in proximity of the transition. As far as the electromagnetic coupling is concerned, the planar transmission line at the common port of the dielectric duplexer shall be connect to useful transition means able to excite the right electromagnetic mode inside the cavity of the metallic waveguide. Typical waveguide exciting means are probes protruding inside the cavity of the waveguide or apertures in a transverse wall (see **Ref.[1], [2],** and **[3]).** That is, suitable connections have to be provided between the common branch of the T-junction and said probes or apertures.

[0006] As a particular example of waveguide exciting means, the European patent application mentioned at **Ref.[5]** (belonging to the same Assignee of the present invention) shows a microwave circuitry laid down on a fibreglass reinforced resin substrate (FR4) including a microstrip coupled to a rectangular waveguide fixed to the FR4 substrate, as shown in the present **figures 3a, 3b**, and **3c. Fig.3a** shows a top view of the microstrip circuitry of **Ref.[5]** in the zone opposite to the end of the mechanical waveguide. With reference to the **fig.3a** a microstrip 4 is visible on the front face of the FR4 substrate 5 along the longitudinal axis A-A. The microstrip 4 ends with a square patch protruding inside an unmetallized square window at the centre of a metallic square crown 6. The substrate 5 is drilled at the four corners of the crown 6. **Fig.3b** shows the bottom face of the substrate 5. A thick copper layer 7 is laid down on the whole face with the exclusion of a rectangular window placed in correspondence of the unmetallized window of the front side. The copper layer 7 is milled for a certain depth along the contour of the unmetallized rectangular window. **Fig.3c** shows a cross-section of the metallized substrate 5 along the longitudinal axis A-A of **fig.3a**. With reference to **fig.3c** the end of a rectangular waveguide 8 is put in contact with the thick copper layer 7 in the zone of the upper crown 6 and is fixed to the substrate 5 by means of screws penetrating in the four holes in the upper face. The thick copper layer 7 acts as a flange for the mounting of the waveguide 7 which prevents dangerous bends of the dielectric substrate 5 and electromagnetic field distortions in the zone of the crown 6. In the figure is well visible a milled zone 9 of the thick ground plane 7 having an unmetallized zone 10 at the centre. The end wall of the waveguide 8 has a square aperture 8' at the centre put in correspondence of the milled zone 9. The microwave signal travelling on the microstrip 4 is injected inside the cavity of the mechanical waveguide 8 through the square patch, the two opposite dielectric unmetallized windows at the two side of the substrate 5, the milled zone 9 of the thick copper layer 7, and the tract 8' with reduced section of the waveguide 8. The above elements constitute a microstrip to waveguide transition, and vice versa, that transforms the "quasi-TEM" propagation mode of the microstrip 4 into the TE_{10} mode of the rectangular waveguide 8.

[0007] The patented embodiment of this citation is not specifically designed for a duplexer , although could be arranged for a filter, nonetheless it provides a sound example of how a microstrip is coupled to a mechanical waveguide through an aperture in a transverse wall (the end wall). Microstrip 4 is essential in case the circuitry on the upper face **(fig.3a)** is a filter because allows to connect the filter to the transition zone towards the mechanical waveguide. The sound example of this citation is unsuitable for alumina substrates because alumina is too brittle to replace the FR4 substrate and doesn't bear to be screwed.

OBJECTS OF THE INVENTION

[0008] The object of the present invention is that to indicate a dielectric duplexer suitable to be connected to a mechanical waveguide in an extremely compact and efficient way.

[0009] Other object of the present invention is that to indicate an method for designing a microwave duplexer filter with the aforementioned characteristics.

SUMMARY AND ADVANTAGES OF THE INVENTION

[0010] To achieve said object the subject of the present invention is a duplexer filter, as disclosed in the relevant claims. The duplexer filter of the invention is constituted by a metallized substrate of alumina interposed between a robust metallic base and a metallic hollow body milled as a short waveguide fixed to the metallic base. The free end of the hollow body is connected to an R140 mechanical waveguide connected to the antenna feeder at the other end. The metallized layout of the alumina substrate has been developed from a dielectric filter previously designed in the laboratories of the same Assignee. This filter, shown in **fig.4**, refers to **Ref. [6]** which is incorporated by reference in the present disclosure. The kind of modifications to the layout of the previous filter are immediately understandable by the comparison of **fig.5** with the preceding **fig.4**. Roughly speaking, the known layout of **fig.4** has been cut out along the transversal axis and the two halves kept separated by an unmetallized dielectric gap on the front face of the same alumina substrate. Each filter is obviously redesigned to reshape the original bandpass in the new frequency bands. Without limiting the invention, the ref-

erence to the filter at **Ref.[6]** only depends on some similarities in the two tapers and in the steps of manufacturing the metallized substrate,. The metallic hollow body includes a terminal tract with reduced section whose rectangular opening is faced to the central unmetallized gap existing between the two dielectric resonant cavities of the two bandpass filters. The walls of the hollow body delimiting the central opening are soldered (by brazing) to the metallic layout delimiting the central unmetallized gap, in order to keep the dielectric and metallic cavities contiguous to each other. The central part of this structure constitutes an extremely compact T-junction including two identically structured transitions between dielectric and mechanical waveguides, and vice versa. Differently from the known art, the proposed T-junction is completely embodied in a waveguide structure: partially dielectric and partially in air. This embodiment avoids to interpose microstrips to feed the transitions; besides separate excitation means as probes or irises as in the prior art unneeded. The novel embodiment of the T-junction prevents any electromagnetic spurts outside the closed structure of the two transitions.

[0011] In a preferred embodiment of the invention the central unmetallized gap projects itself outside the rectangular profile to optimise the matching of the T-junction and to simplify in the meanwhile the sealing of the space between metallic and dielectric cavities.

[0012] In another embodiment of the invention the tract with reduced section is filled up with a dielectric material having a relative dielectric permittivity comprised between the permittivity of the air and the alumina. This expedient improves the matching of the T junction.

[0013] The disclosed transition can be arranged for coupling a generic dielectric filter, non necessarily of the duplexer type, to a mechanical waveguide. For this aim it's enough to replace one of the two filters with a termination able to provide the right value of admittance in the band of the remaining filter..

[0014] The duplexer of the present invention is advantageously usable in the low or medium capacity digital radio links, so as in the fixed stations of cellular telephone systems exploiting FDD duplexing. Other advantages of the duplexer of the invention are: miniaturisation, great repeatability, no-tuning, direct connection to the antenna, and cost saving.

[0015] Other object of the invention is a method for designing the microwave duplexer filter mentioned above. The whole duplexer is designed step-by-step by an innovative extension of the Guglielmi's method of the **Ref.[7].** This extension is devoted to build up the duplexer filter gradually around a previously consolidated model of the T-junction whose parameters have been obtained pursuing the maximum simultaneous matching at the three ports.

BRIEF DESCRIPTION OF THE DRAWINGS

[0016] The features of the present invention which are considered to be novel are set forth with particularity in the appended claims. The invention, together with further objects and advantages thereof, may be understood with reference to the following detailed description of an embodiment thereof taken in conjunction with the accompanying drawings given for purely non-limiting explanatory purposes and wherein:

- **figures 1** and **2**, already described, show two canonical circuital schemes of a duplexer ;
- **figures 3a, 3b**, and **3c**, already described, show the embodiment of a microstrip to waveguide transition of the known art, relative to an FR4 dielectric substrate;
- **fig.4** shows the photograph of a dielectric filter of the prior art taken as starting point for the design of the present duplexer;
- **figures 5**, and **5a** show two photographs of the top view of simpler one and a preferred embodiment, respectively, of the duplexer of the invention;
- **fig.6** shows the photograph of the metallic base housing the duplexer;
- **figures 7** and **8** show two embodiments of the mechanical body of the duplexer to be joined to the metallic base of fig.6;
- **fig.9** shows the photograph of the ensemble constituted by the base plus the metallic body of the duplexer;
- **fig.10** shows an exploded view of the mechanical ensemble of fig.9, partially sectioned;
- **fig.11** shows a cross-section along the axis B-B of the ensemble of fig.10;
- **figures 12a** shows a tridimensional view of a basic model of the T-junction referred to the layout of fig. 5 and recognizable in the central part of fig.11;
- **figures 12b**, and **12c** show two cross sections of the T-junction of fig.12a;
- **figures 13a** to **13k** show as many matching curves at the ports of the T-junction of fig.12a relevant to the various design steps;
- **figures 14a** shows a model of a tapered transition visible in the layout of figures 5 and 5a;
- **figures 14b,** and **14c** show the configuration of the electric field relatively to a microstrip and a dielectric waveguide respectively connected at the two ends of the tapered transition of fig.14a;
- **fig.14d** shows a curve of the reflection coefficient measured at the microstrip input of the tapered transitions of the preceding figures;
- **fig.15** shows a tridimensional view of a basic model of the preferred T-junction referred to the layout of fig.5a;
- **figures 16a, 16b,** and **16c** show as many matching curves of the T-junction of fig.15 relevant to the various design steps;

- **fig.17** shows a tridimensional view of an upgrade of the model of fig.15 useful for dimensioning first resonant tracts of the two filters at the two sides;
- **fig.18** shows matching curves of the model of fig. 17;
- **fig.19** shows a top view of the model of fig.17 completed with second resonant tracts;
- **figures 20a** and **20b** show initial and final matching curves of the model of fig.19;
- **fig.20c** shows the transmission and reflection curves at the ports of the duplexer filter of the present invention.

DETAILED DESCRIPTION OF AN EMBODIMENT OF THE INVENTION

[0017] With reference to **fig.4** we see in detail the starting point filter of **Ref.[6]** for designing the duplexer. The bandpass filter of **Ref.[6]** is embodied as a rectangular dielectric waveguide (GDL-RIS) obtained by opportunely metallizing an alumina substrate. The metallization cover: the whole surface of the back side, the longitudinal lateral walls in correspondence of the dielectric waveguide, and the front side in correspondence of the dielectric waveguide and two identical input/output transition structures that include tapers and microstrips. The dielectric waveguide behaves as a resonant cavity having bandpass response. Some metallized through holes with opportune diameters are spaced $\lambda_G/2$ to each other inside the dielectric resonant cavity. The holes act as inductive "posts" for modelling as desired the frequency response (200 MHz bandwidth at 7.6 GHz). Two caves are dug in the substrate and metallized to obtain the longitudinal side walls of the resonant cavity. Successively the filter is separated from the substrate by cutting the substrate along the centre-line of the metallized caves. An industrial laser is profitably used to dig the caves and saw the substrate. Alternatively a diamond saw can be used for the last operation. Each input/output structure to/from the dielectric guide is a microstrip which enlarge itself progressively with linear low as gradually approaches the resonant cavity. The specific geometry behaves as a tapered transition between the quasi-TEM propagation mode of the electromagnetic signal through the microstrip and the dominant TE_{10} mode of the dielectric guide, or vice versa. In the same time each transition adapts inside the bandpass of the filter the 50 Ohm impedance of the microstrip to the impedance seen at the respective ports of the dielectric resonant cavity. Thanks to the high precision of the manufacturing process the tuning operation is made unnecessary.

[0018] **Fig.5** shows the front-side of an alumina substrate 11 metallized in correspondence of two bandpass filters BPL and BPH separated by an unmetallized central gap GP. The location of the BPL and BPH filters at the two halves of the alumina substrate 11 is immaterial. In the following the BPL filter is named "low" and the BPH filter "high" due to the different location of the respective bands. The association of the TX and RX filters either to the BPL or BPH depends on the specification of the transmission system. Differently from the symmetric layout of **fig.4** each filter of **fig.5** is comparable to either the even or the right half. The BPL filter includes a microstrip MSL connected to a tapered transition TPL towards a dielectric resonant cavity CVL delimited by the central gap GP. Three metallized through holes P1L, P2L, and P3L with different diameters and positions are visible in the dielectric cavity BPL. Similarly the BPH filter includes a microstrip MSH connected to a tapered transition TPH towards a dielectric resonant cavity CVH delimited by the central gap GP. Three metallized through holes P1H, P2H, and P3H with different diameters and positions are visible in the dielectric cavity BPH. The bottom face of the alumina substrate 11 is completely metallized, while the longitudinal side walls are metallized in correspondence of the two resonant cavities and the central gap GP. The layout visible in **fig. 5a** is relevant to a preferred embodiment in which the alumina substrate 11 in correspondence of the central unmetallized gap GP is larger than the remaining part and is surrounded by a narrow metallized frame which continues perpendicularly on the side walls reaching the metallized back face, in order to shield the gap GP laterally. It is useful point out that the two shorter edges of said narrow frame are constituting two metallized strips 12 and 13 which delimit gap GP transversally. A not completely shielded version of the gap GP (visible in fig. 6) includes the only two metallized strips 12 and 13. The metallized holes have the function of inductive posts as already said in the description of **fig.4.**

[0019] **Fig.6** shows a thick metallic base 14 of the duplexer with the metallized alumina substrate 11 of the preceding **fig.5a** soldered at the centre-line by means of a preformed layout (visible in the successive fig.10). The base 14 has rectangular form with two thick fins 15 at the shorter sides for giving support to two SMA connectors. Four hollow cylindrical pins 16, threaded at their inside along the longitudinal axis, are visible at the four corners of the base 9. The cylindrical pins 16 have in the bottom a hexagonal head 16' upon a threaded lower extension (not visible) screwed into the metal of the base 9.

[0020] **Fig.7** shows a metallic body 17 with four holes at the corners for housing the cylindrical pins 16 (fig.6) and a rectangular window MC-T opened in a rectangular projection 17a at the centre, having a groove in correspondence of the opening MC-T for housing the metallized alumina substrate depicted in **fig.5.** When pins 16 are inserted into the corresponding holes of the metallic body 17 the opening MC-T is faced to the dielectric gap GP, shape and dimensions of MC-T and GP are the same.

[0021] **Fig.8** shows a metallic body 17 which differs from the previous one mainly because the central rectangular projection 17b is flat and the rectangular aper-

ture MC-T is a little longer than the previous one to match the wider gap GP of the metallized alumina substrate depicted in **fig.5a**.

[0022] **Fig.9** shows the ensemble of the metallic body 17 mounted on the metallic base 14 with the interposed alumina 11. The metallic body 17 is kept detached from the base 14 by the thickness of the hexagonal heads 16' of the cylindrical pins 16, avoiding of breaking the alumina 11. The metallic body 17 has a central opening MC-G in correspondence of the opening MC-T on the opposite face. The two openings MC-G and MC-T are the ones of two contiguous homonym rectangular cavities dig through the thickness of the metallic body 17.

[0023] **Fig.10** shows an exploded view of the assembly of the preceding **fig.9** where corresponding elements of the preceding figures are indicated with the same labels. With reference to **fig.10** a preformed layout 18 is in interposed between the metallic base 14 and the dielectric substrate 11. Two preformed tablets 19 are posed in contact with the upper metallization of the two resonant cavities CVL and CVH at the two sides of the dielectric gap GP. Two other preformed tablets 20 are placed sideways the two shorter sides of the gap GP. The central conductors of the two SMA connectors have an unshielded pin 21 soldered to the microstrip MSL and MSH, respectively.

[0024] **Fig.11** shows a cross-section taken along the plane **B-B** of the preceding **fig.10** highlighting the ensemble of the duplexer connected to an R140 waveguide and to the two SMA connectors. The duplexer filter includes the mechanical base 14, the metallized alumina 11 with the central gap GP and the metallized through holes, the preformed elements 18, 19 and 20, and the upper metallic body 17 including the contiguous cavities MC-G and MC-T. With reference to **fig.11** we see that the four cylindrical pins 16 keep the mechanical part of the T-junction and an R140 guide centred on the dielectric gap GP, avoid in the meanwhile the alumina substrate 11 is pressed against the base 14 the by the metallic body 17 and broken consequently. The space between the MC-T air cavity and the alumina substrate 11 is sealed by the preforms 19 and 20. The preforms are constituted by an AuSn alloy having a melting point lower than the golden layout of the two filters. When the mechanical ensemble of the duplexer is heated slightly over the melting point of the AuSn alloy, the preforms 18, 19 and 20 melt down and the alumina layout is fused to the mechanical parts 14 and 17. This technique is known as brazing. Mechanical parts 14 and 17 are finished with gold for the welding aim other than the reduction of the resistive losses.

[0025] The duplexer design of the embodiment of **fig. 5** is discussed first and successively will be discussed the preferred embodiment of **fig.5a**. From the electromagnetic point of view the duplexer of the previous **figures 4** to **11** is a particular three-port circuit comprising:

- a T-junction including two identically structured transitions between the rectangular air cavity MC-T of the metallic hollow body 17 and the two opposite dielectric cavities CVL and CVH of the alumina substrate 11. The T-junction is the most innovative element of the duplexer but also the most critical ones; it is completely embodied in waveguide structure: partially dielectric and partially in the air. Both the cavities of the two type of waveguides bear a fundamental TE_{101} mode. The two coplanar dielectrics resonant cavities are orthogonal to the metallic cavity, so that the lines of the electric field are forced to rotate of 90° inside the thickness of the dielectric gap GP in proximity of the two right corners..
- the two bandpass filters BPL and BPH built up on said dielectric cavities;
- the two tapered transitions TPL and TPH between said dielectric cavities and the two microstrips MSL and MSH laid down on the same alumina substrate 11 for the connection to other circuits.

[0026] From the theoretical point of view it's useful to remind that a three port junction (T-junction) can't be simultaneously isotropous (reciprocal), no-losses, and adapted at the three ports. This fact prevents from the application of traditional methods to design the two bandpass filters. Following traditional methods the filters shall be closed on a standard impedance (50 Ohm) at the ends, but when they are connected to the T-junction the junction cannot operate optimally because of the aforementioned restrictions. From the practical point of view the mechanical part of the T-junction has greater tolerances than the dielectric parts, due to the different precisions of the two manufacturing processes. Performance optimisation of an T-junction shall pursue a trade-off between the best electrical matching at the various ports and the simplest mechanical implementation. The whole duplexer is designed step-by-step by an extension of the Guglielmi's method of the **Ref.[7]**. The focus of the method is that to pursue at each designing step the best matching between the response of a microwave theoretical filter and a partial embodiment of the corresponding real filter obtained by an efficient software package for the full-wave simulation of filter structures. Guglielmi's method has been adapted to the duplexer design as it results by the following steps that will be detailed:

- designing the T-junction at first;
- connecting first resonant tracts of the two dielectric cavities CVL and CVH at the two branches of the T-junction and optimising the overall response by acting on the only parameters of the two first resonant tracts;
- connecting second resonant tracts of the two dielectric cavities CVL and CVH to the first consolidated tracts and optimising the overall response by acting on the only parameters of the second resonant tracts;

- and so forth for all the resonant tracts;
- connecting the two tapered transitions to the two last consolidated tracts and optimising the overall response by acting on the only parameters of the two tapered transitions. A profitable alternative is that of dimensioning the two last resonant tracts together with their tapered transitions simultaneously.

[0027] Differently from the conventional methods, the two filters are now designed by progressively modelling them on the T-junction they are connected to. A certain grade of freedom exists in the design to delimit the boundaries of the dielectric resonant tracts of the filters depicted in **fig.5**. In the pursuit of the best matching either adaptation or frequency responses can be considered; presently adaptation has been considered.

[0028] **Fig.12a** shows an ideal model of the T-junction suitable for the dielectric metallized substrate of **fig.5** in which the long branch (vertical) of the T structure coincides with the two contiguous air cavities MC-T and MC-G of the metallic body 17; the two short branches of the T coincide with two short tracts of the two dielectric waveguides at the two sides of the unmetallized gap GP; and the common point of the three branches of the T-junction coincides with the thickness of the unmetallized gap GP. The ensemble of these elements constitutes a double dielectric-waveguide to air-waveguide transition, and vice versa. **Fig.12b,** and **12c** show two cross sections of the basic model of **fig.12a** taken along the longitudinal axis **B-B** and the transversal axis **C-C**, respectively. Once the structure of the T-junction is planned, the design criterion is that to obtain the maximum simultaneous matching a the three ports indicated in **fig.12a** as PORT 1, PORT 2, and PORT 3. Relevant parameters to be varied for optimising the structure are the following:

h_G_air is the height of the MC-G cavity (R140);
w_G_air is the width of the MC-G cavity (R140);
w_T_air is the width of the MC-T cavity also equal to the length of the gap GP;
h_T_air is the height of the MC-T cavity;
w_alu_centr is the width of the central unmetallized gap GP of the alumina substrate;
1_alu_low is the length of a dielectric waveguide bit belonging to the branch of the T-junction connected to the low filter (bandpass);
1_alu_high is the length of a dielectric waveguide bit belonging to the branch of the T-junction connected to the high filter (bandpass);

[0029] The area of the rectangular gap GP, corresponding to the area of the opening MC-T is: (w_T_air $\times$ w_alu_centr). Discontinuities on the path of the RF signal at the common point of the three branches of the T-junction are the most critical propagation zones corresponding to the transition from the air to dielectric waveguide, and vice versa. The maximum simultaneous matching a the three ports is obtained step-by-step starting from values taken empirically, and also considering the known design of the departure filter of fig.4. The first step is the optimisation of the h_T_air parameter considering the following departure values:

w_G_air = R140 standard;
h_G_air = 1 mm (immaterial above a minimum requested for simulation aim);
h_T_air = 0.5 mm;
w_T_air = 0.5 mm;
w_alu_centr = 15.798 mm;
1_alu_low = 0 mm;
1_alu_high = 0 mm;
The thickness of the alumina substrate is 0.635 mm;
the thickness of the metallic layers is 7 μm.

[0030] The h_T_air parameter is varied with steps of 1 mm and at each step the matching at the three ports is checked by evaluating the scattering parameters S11, S22, and S33. **Fig.13a** shows the scattering coefficient S11 module versus frequency for each optimisation step. The best matching is for h_T_air = 5 mm. The S22 and S33 curves in correspondence of this value are visible in **fig.13b.**

[0031] The second step is the optimisation of the w_T_air parameter considering the departure values of the first step in which w_T_air is varied from 0.5 to 2.5 mm, with 0.5 mm steps, and h_T_air = 5 mm. **Fig.13c** shows the scattering coefficient S11 module versus frequency for each optimisation step. Best results are obtained for $1.5 \leq$ w_T_air ≤ 2 mm. To avoid excessive resistive losses the compromise value of 2 mm is chosen. The S22 and S33 curves in correspondence of this value are visible in **fig.13d.**

[0032] The third step is the optimisation of the parameter w_alu_centr after considering as consolidated the values at the end of second step. The parameter w_alu_centr is reduced from 15.798 to 5.046 mm, with 2 mm steps. **Fig.13e** shows the module versus frequency of the scattering coefficient S11 for each optimisation step. Unfortunately the value of 5.046 mm which minimises the area of the alumina doesn't allow the best optimisation. This drawback is remedied by the preferred embodiment of **fig.5a.** The S22 and S33 curves in correspondence of the 5.046 mm value are visible in **fig. 13f.**

[0033] The fourth step is the optimisation of the 1_alu_low and 1_alu_high parameters considering as consolidated the values at the end of third step. The parameters 1_alu_low = 1_alu_high are varied fro 0 to 4 mm with 1 mm steps. **Fig.13g** shows insignificant variations between the curves of the module versus frequency of scattering coefficient S11. Considering the effective distance between the first inductive posts P1L, PIH and the two respective sides of gap GP as more significant parameters than the physical lengths 1_alu_low and 1_alu_high, a 2 mm compromise value is chosen to have not troubles with the drilling of said

posts. The S22 and S33 curves in correspondence of 2 mm value are visible in **fig.13h.**

[0034] The fifth step is the optimisation of the h_G_air parameter considering as consolidated the values at the end of fourth step. The parameter h_G_air is varied from 1 to 7 mm with 2 mm steps. **Fig.13i** shows insignificant variations of the scattering coefficient S11 module versus frequency above 2 mm height. The parameter h_G_air only influences the difference into the phase-offsets of the two filters. After assuming h_G_air = 5 mm, the S11, S22 and S33 curves are visible in **fig.13j.** As far as the frequency response of the T-junction is concerned, the curves depicted in **fig.13j** show that this response is centred around a frequency of 15.6 GHz. At this point the T-junction is ready to interconnect the "high" and "low" bandpass dielectric filters.

[0035] The sixth step is devoted to the dimensioning of the two bandpass filters of the duplexer. For this aim the bands of the "high" and "low" filters are placed at the two sides of the 15.6 GHz frequency line. In order to simplify the design each filter has a second order Chebyshev response obtained with two resonant tracts. In respect of higher order filters the out-of-band performances are relaxed, without limiting the invention. The following specifications are assumed:

LOW BANDPASS FILTER

[0036]

f_{OL} = 15.300 GHz
B = 120 *MHz*
Rloss = 25 dB
α = *10 dB*
f_{α} = 668.5 MHz

HIGH BANDPASS FILTER

[0037]

f_{OL} = 16. 100 *GHz*
B = 120 *MHz*
Rloss = 25 dB
α = *10 dB*
f_{α} = 668.5 MHz

[0038] As previously said the two dielectric "high" and "low" bandpass filters are designed by an extension of the Guglielmi's method indicated at **Ref.[7]**. The application of this method presupposes the knowledge of the frequency responses of the canonical model chosen to represent the BPL and BPH filters. A first substep 6.1 is devoted to this aim. The two ideal curves of the scattering coefficient S11 are shown in **fig.13k** and **fig.131** for the one-resonator and two-resonator filters, respectively. In the latter case the return loss specifications are marked on the curves. A commercial software package named WIND is usable for this aim.

[0039] A second substep 6.2 is devoted to optimise the physic parameters of the first resonant tracts connected to the two horizontal branches of the consolidated T-junction. For design convenience the first resonant tracts include the pair of posts adjacent to the gap GP; namely the P1L, P2L posts of the cavity CVL and the P1H, P2H posts of the cavity CVH. The parameter to be optimised are the following: D1_L, D1_H, D2_L, D2_H, disp1_L, disp1_H, cav1_L, and cav1_H, where: D1_L is the diameter of the hole P1L; D1_H is the diameter of the hole P1H; D2_L is the diameter of the hole P2L; D2_H is the diameter of the hole P2H; disp1_L is the displacement of the hole D1_L from the centre-line of the alumina; disp1_H is the displacement of the hole D1_H from the centre-line; disp2_L is the displacement of the hole D2_L from the centre-line; disp2_H is the displacement of the hole D2_H from the centre-line; 1_cav1_L is the length of the first resonant tract of the cavity CVL including the two posts P1L and P2L; and 1_cav1_H is the length of the first resonant tract of the cavity CVH including the two posts P1H and P2H. The starting values of these parameters are achievable by empirical considerations or calculated as indicated in the Marcuvitz book at **Ref.[2].** Adopting the empirical criterion a poor matching is reached and the parameters shall be successively changed having the following concepts in mind:

- reducing the diameters of first posts P1L and P1H is equivalent to increase the effective lengths 1_cav1_L and 1_cav1_H of the first resonant tracts. The frequency responses of the two filters translate towards the low and the band is widened. Besides the electromagnetic coupling increases and the reflection coefficient S11(f) decreases.
- Increasing the diameters of second posts P2L and P2H is equivalent to reduce the effective lengths 1_cav1_L and 1_cav1_H of the first resonant tracts. The frequency responses of the two filters translate towards the high and the band is slightly narrowed. Besides the electromagnetic coupling decreases and the reflection coefficient S11(f) increases.
- Keeping the diameters of the first and second posts constant but increasing the lengths of first resonant tracts, the frequency responses translate towards the low.

The final values of the parameters of the two resonant tracts will be given for the preferred embodiment of the variant of **fig.5a**, described later on. Nowadays powerful simulation software tools exist in commerce to prevent the direct calculation of the structure.

[0040] A third substep 6.3 is devoted to optimise the physic parameters of the second resonant tracts connected to the first consolidated one. The second resonant tracts include the third post P3L and P3H of the cavity CVL and CVH, respectively. The parameter to be

optimised are the following: D3_L, D3_H, disp3_L, disp3_H, cav3_L, and cav3_H, where: D3_L is the diameter of the hole P3L; D3_H is the diameter of the hole P3H; disp3_L is the displacement of the hole D3_L from the centre-line of the alumina; disp3_H is the displacement of the hole D3_H from the centre-line; 1_cav3_L is the length of the second resonant tract of the cavity CVL including the post P3L; and 1_cav3_H is the length of the second resonant tract of the cavity CVH including the post P3H. As previously said, a joined dimensioning of the second resonant tracts together with their tapered transitions TPL and TPH is advantageously achievable in the third substep 6.3. A tapered layout is visible in **Fig. 14a** where a transversal plane indicates the begin/end of the taper. **Fig.14b** shows the configuration of the electric field through the alumina substrate, and the upper air space, in correspondence of the microstrips MSL and MSH (fig.5). **Fig.14c** shows the configuration of the electric field inside the dielectric waveguide CVL and CVH (fig.5). The resemblance between the two configurations demonstrate a reciprocal compatibility between the two structures, so that a simple transformation of the impedance passing from the one to the other structure can be achieved consequently. As disclosed in **Ref.[6]** the linear taper is the most suitable geometry for gradually transforming the electric field from the one to the other structure. **Fig.14d** shows a curve of the reflection coefficient measured at the microstrip input of the tapered transitions.

[0041] The starting values of the parameters which describe second resonant tracts and the respective tapers are achievable by empirical considerations or calculated as indicated in **Ref.[2]** and **Ref.[6],** assuming w = 0,60 mm the width of the two microstrips MSL and MSH (fig.5) and 50 Ohm their characteristic impedance. In any case a poor matching is achieved with the initial parameters and they shall be successively changed having the following concepts in mind:

- reducing the diameter of third posts P3L and P3H is equivalent to increase the flow of the electrical field towards the external of second resonant tracts. A higher coupling between the filter and the microstrip is achieved consequently.
- Reducing the length of second resonant tracts the frequency responses translate towards the high and the two bands are slightly widened.

[0042] The simulation results confirm the design approach of the substep 6.3. In fact the matching of the tapered transition is greater than 20 dB into the optimal band centred around 15.6 GHz.

[0043] Now some modifications of the previous design is considered for implementing a preferred embodiment of the invention. The aim is that to improve the optimisation of the T-junction without increasing the consumption of the alumina. For this aim both the alumina and the mechanics are modified with respect to the original design. More precisely, with reference to **fig.5a** the coupling area of the alumina substrate 11 is increased in correspondence of the gap GP and the light of the opening MC-T is enlarged of the same amount **(fig.8).** From the implementation point of view the central gap GP has been extended outside the original profile and the central projection including the opening MC-T is made flat (fig.8) to be put in contact with the alumina surface. The complicated insertion of the small preforms 20 for closing the junction laterally is prevented thanks to the introduced modifications. Now the preforms 20 are placed on the metallized lips 12 and 13 directly. The enlargement of the gap GP is established by the distance w_alu_centr between the two metallized lips 12 and 13. Some modifications shall be introduced into the basic model of the T-junction of **fig.12a** in order to support the new design of the preferred embodiment. The modified basic model is depicted in **fig.15.** From the comparison of the two models we see an additional metallic thickness at the base of the vertical branch of the T-junction; furthermore the ideal rectangular shape is leaved in favour of a more realistic shape where the corners are rounded off. A so drastic modification of the T-junction, without any redesign, unavoidably would impact on the previously optimised electrical behaviour. In particular, the matching curves of the S11 coefficient should be shifted near 17 GHz upwards, as shown in **fig. 16a.** A new optimisation of the T-junction is pursued to let the previous 15.6 GHz frequency unchanged; this allows to keep the central frequencies of the two filters also unchanged, minimising their redesign to match the new T-junction. The performed strategy is the following:

- the parameter h_T_air is reduced for translating the curves of **fig.16a** downwards until the 15.6 GHz is newly centred;
- the parameter w_alu_centr is increased for augmenting the matching until the original 6 dB matching is restored;
- the other parameters are unchanged with respect to the preceding design.

[0044] The optimisation steps are listed below, where the parameters modified at each step are indicated in bold. The relative curves of the S11 coefficient are reported in **fig.16b** and the final result is shown in **Fig.16c.**

(1) w_alu_centr = 5.046 mm; h_T_air = 4.15 mm
(2) w_alu_centr = 5.046 mm; **h_T_air** = **4.85** mm
(3) **w_alu_centr = 7.046** mm; h_T_air = 4.85 mm
(4) w_alu_centr = 7.046 mm; **h_T_air = 4.60 mm**
(5) **w_alu_centr = 7.446 mm; h_T_air = 4.50 mm**

[0045] The mechanical characteristics of the T-junction are changed quite a lot but the electrical behaviour has been bring back to the original one. In first approximation the old filters are still usable; nevertheless their redesign is advisable. The Guglielmi's method is applied

to the model visible in **fig.17** that includes first resonators connected to the T-junction. In the first optimisation step the initial parameters of the first resonator listed below have been obtained, taking into considerations the values of the first design:

D1_H = 0.80 mm
D2_H = 1.37 mm
D1_L = 0.63 mm
D2_L = 1.24 mm
cav1_H = 3.64 mm
cav1_L = 3.71 mm
disp1_H = 1.56 mm
disp2_H = 2.53 mm
disp1_L = 1.32 mm
disp2_L = 2.53 mm

[0046] With these parameters the S11 responses of the two filters are checked and compared with the ideal responses in **fig.18.** The figure shows a good matching between the two curves, nonetheless a further improvement is pursued modifying the individual parameters until micrometric precision is reached. The final values are the following:

D1_H = 0.80 mm
D2_H = 1.355 mm
D1_L = 0.641 mm
D2_L = 1.233 mm
cav1_H = 3.665 mm
cav1_L = 3.70 mm
disp1_H = 1.56 mm
disp2_H = 2.53 mm
disp1_L = 1.32 mm
disp2_L = 2.53 mm

The final responses are a bit more steep than the ones of **fig.18** and are not represented for the sake of simplicity.

[0047] With reference to **fig.19** the second resonant tract is introduced in the basic model and the complete duplexer is obtained. In the first optimisation step of the second resonant tract the initial parameters of this tract listed below are obtained, taking into considerations the values of the first design:

D3_H = 0.74 mm
D3_L = 0.60 mm
disp3_H = 2.523 mm
disp3_L = 2.523 mm
cav2_H = 3.953 mm
cav2_L = 4.148 mm

[0048] With reference to **fig.20a** the S11 responses of the two filters embodied with the listed parameters are checked and compared with the ideal responses. The agreement is not satisfactory and the optimisation process must be continued. Up to six optimisation steps are performed but for the sake of simplicity the relative figures are not considered. More precisely: in the second step D3_L diameter and cav2_L length are reduced for increasing the coupling of the second with the first resonant tract of the low filter. More than 5 dB of matching is gained. In the successive third and fourth steps the same is performed for the second resonant tract of the high filter, achieving good results. It is possible conclude that the initial diameters were excessive. In the fifth and sixth steps the high and low filters are further improved by introducing micrometrical corrections. The final values are the following:

D3_H = 0.68 mm
D3_L = 0.58 mm
disp3__H = 2.523 mm
disp3_L = 2.523 mm
cav2_H = 3.935 mm
cav2_L = 4.09 mm

[0049] With reference to **fig.20b** the S11 responses of the two filters embodied with the final parameters are checked and compared with the ideal responses. The agreement is satisfactory and the optimisation process is terminated. The ultimate **fig.20c** shows three relevant scattering parameters S11, S21, and S31 of the complete duplexer.

BIBLIOGRAPHY

[0050]

[1] "Microwave Filters, Impedance-Matching Networks, and Coupling Structures"; G.L.Matthaei, L. Yong and E. M. T. Jones; Artech House Books; 1980.

[2] "Waveguide Handbook; N. Marcuvitz; McGraw-Hill Book Company; 1951.

[3] "Foundation for Microwave Engineering"; R. E. Collin; McGraw-Hill 2nd Edition; © 1992.

[4] "26 GHz $TM_{11\delta}$ Mode Dielectric Resonator Filter and Duplexer with High-Q Performance and Compact Configuration"; Akira Enokihara et al.; 2002 IEEE MTT-S International Microwave Symposium Digest (Cat. No.02CH37278) IS: ISBN 0-7803-7239-5L; Seattle, WA USA; 2-7 June 2002.

[5] European patent application Number: EP 02425349.4; titled: "BROADBAND MICROSTRIP TO WAVEGUIDE TRANSITION ON MULTILAYER PRINTED CIRCUIT BOARDS ARRANGED FOR OPERATING IN THE MICROWAVES" priority 30-05-2002; inventors: Carlo BUOLI, Aldo BONZI, Vito Marco GADALETA, Tommaso TURILLO, Alessandro ZINGIRIAN; priority 30-05-2002.

[6] European patent application Number: EP 03007045.2; titled: "FILTRO NON SINTONIZZABILE IN GUIDA D'ONDA DIELETTRICA RETTANGOLARE"; inventors: BONATO, CARCANO, DE

MARON, GAIANI, MORGIA; Patent Assignee SIEMENS ICN; priority 27-06-2002 "Novel design procedure for microwave filters";
[7] M. Guglielmi and A. Alvarez Melcon; 23rd European Microwave Conference, pp. 212-213, Madrid, Spain, 1993.

Claims

1. A microwave duplexer filter comprising two dielectric bandpass filters with separated bands, each filter being connected to a respective first or second port of a three-port coupler, named T-junction in the following, and to a microstrip conveying either a transmission or reception signal, a third port of the T-junction being connected to bidirectional means towards the antenna feeder, **characterised in that** includes:

   - a single dielectric substrate (11) opportunely metallized on the two opposite faces, conventionally named front and back, and laterally for obtaining two dielectric resonant cavities (CVL, CVH) relevant to said bandpass filters (BPL, BPH) located at the two sides of a central unmetallized gap (GP) on the front face;
   - a metallic hollow body (17) like a short rectangular waveguide superimposed to the alumina substrate (11) in a way that its opening (MC-T) is faced to said central unmetallized gap (GP) and its walls are in contact with the metallic layout delimiting said gap (GP) for keeping said dielectric cavities (CVL, CVH) and the metallic cavity (MC-T) of the hollow body (17) contiguous to each other to form said T-junction having said third port in correspondence of the free end of the metallic hollow body (17).

2. The microwave duplexer filter according to claim 1, **characterized in that** the first and second ports of the T-junction which the dielectric bandpass filters are connected to are located inside the dielectric resonant cavities (CVL, CVH) of the respective filters at the end of a short tract from the two sides of said central unmetallized gap (GP), and the two short tracts constituting two aligned branches of the T-junction whose right angle branch is constituted by said metallic hollow body (17).

3. The microwave duplexer filter according to claim 1 or 2, **characterized in that** said metallic hollow body (17) includes a first tract with reduced cross-section (MC-T) faced to said central unmetallized gap (GP), the shape and dimensions of said reduced cross-section being equal to the shape and dimensions of said unmetallized gap (GP), and a second tract (MC-G) with standard section connected to a rectangular waveguide towards the antenna feeder.

4. The microwave duplexer filter according to one of the preceding claims, **characterized in that** includes preforming metallic means (19, 20) for closing the T-junction around said central unmetallized gap (GP).

5. The microwave duplexer filter according to one of the preceding claims, **characterized in that** in correspondence of said central unmetallized gap (GP) the dielectric substrate (11) enlarges outward the remaining profile at the two sides for optimising the matching at the ports of the T-junction.

6. The microwave duplexer filter according to the preceding claim, **characterized in that** includes a narrow metallized frame around said enlarged central unmetallized gap (GP) whose metallization extends on the perpendicular side walls reaching the metallized back face, in order to shield the gap (GP), and the two shorter edges (12, 13) of said narrow metallized frame giving support to said preforming metallic means (20).

7. The microwave duplexer filter according to one of the preceding claims, **characterized in that** includes a metallic base (14) for bearing said single metallized dielectric substrate (11) and the superimposed metallic hollow body (17) .

8. The microwave duplexer filter according to the preceding claim, **characterized in that** said metallic base (14) comprises means (16, 16') for tightening said metallic hollow body (17) without pressing the surface of said metallized dielectric substrate (11) in correspondence of said central unmetallized gap (GP).

9. The microwave duplexer filter according to one of the preceding claims, **characterized in that** said tract with reduced cross-section (MC-T) of said metallic hollow body (17) is filled up with a dielectric material having a relative dielectric permittivity comprised between the permittivity of the air and the alumina substrate.

10. The microwave duplexer filter according to one of the preceding claims, **characterized in that** said dielectric resonant cavities (CVL, CVH) relevant to said bandpass filters (BPL, BPH) include metallized through holes (P1L, P2L, P3L; P1H, P2H, P3H) acting as inductive posts for shaping the separate bandpass responses in a no-tuning way.

11. The microwave duplexer filter according to one of the preceding claims, **characterized in that** said

microstrips (MSL, MSH) conveying either a transmission or reception signal are connected to the respective dielectric resonant cavities (CVL, CVH) by means of a tapered layout (TPL, TPH).

12. Method for designing the microwave duplexer filter of the claim 1, **characterized in that** includes the steps of:

a) building up a model of the T-junction in accordance with at least the following parameters: the cavity height (h_T_air) of the metallic hollow body (17), the width (w_T_air) of the cross-section of the metallic hollow body (17) corresponding to the length of the unmetallized gap (GP), the width (w_alu_centr) of the unmetallized gap (GP), the length (1_alu_low, 1_alu_high) of an short tract of each two dielectric resonant cavities (CVL, CVH) departing from the two sides of the central unmetallized gap (GP);
b) assigning initial empirical values at said parameters of the T-junction;
c) varying step-by-step inside a predetermined range the cavity height (h_T_air) of the metallic hollow body (17) starting from said initial value and for each step measuring or calculating the reflection coefficient at each port of the T-junction and selecting the value giving maximum simultaneous matching a the three ports and considering as consolidated the optimised value;
d) repeating the optimisation step like the preceding one for all the remaining parameters of the T-junction;
e) upgrading the consolidated T-junction model with the model of a first resonant tract of the two dielectric resonant cavities (CVL, CVH) belonging to the bandpass filters (BPL, BPH) and varying step-by-step the parameters of the only said first resonant tracts for pursuing the best matching between the response of a microwave canonical duplexer filter and the response of the above upgraded model obtained by a commercial software package for the simulation of filter structures;
f) repeating the optimisation step like the preceding one for all the remaining resonant tracts of the two dielectric resonant cavities (CVL, CVH) belonging to the two bandpass filters (BPL, BPH).

13. The method of the preceding claim, **characterised in that** the model of the duplexer is upgraded for including the two last resonant tracts of the dielectric resonant cavities (CVL, CVH) integrated with the model of two respective tapered layout (TPL, TPH) towards microstrips (MSL, MSH) conveying a transmission or reception signal.

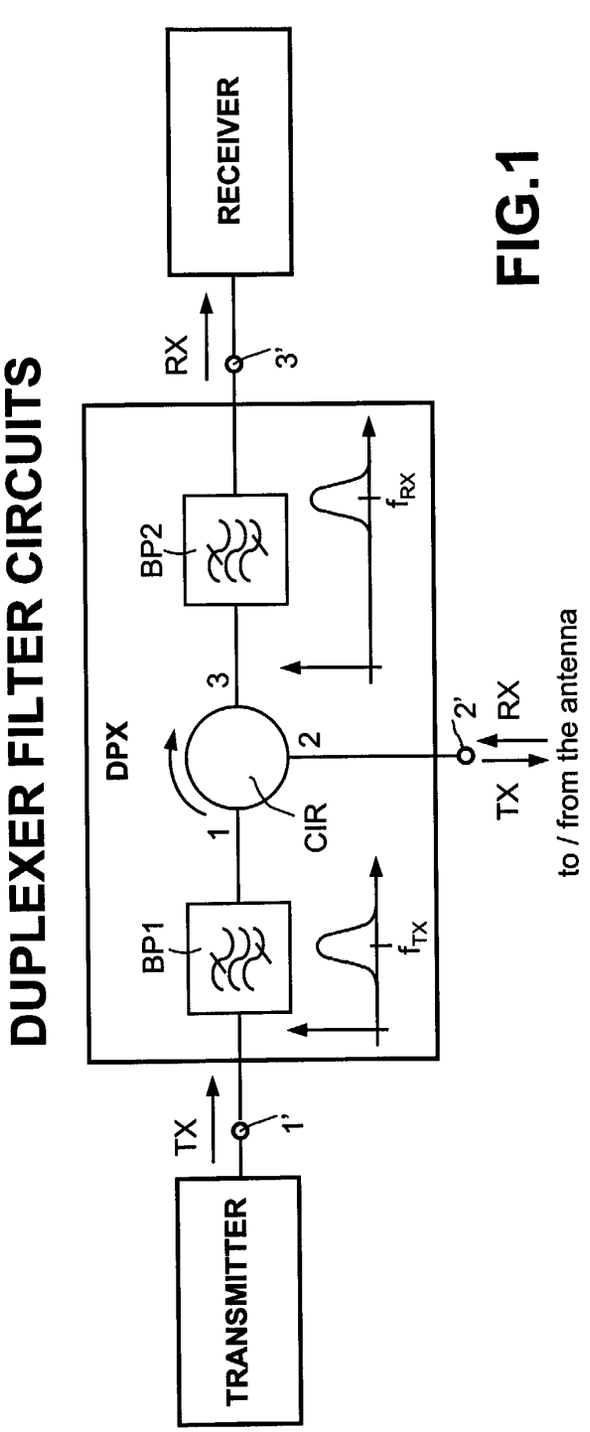
DUPLEXER FILTER CIRCUITS
TRANSMITTER
RECEIVER
TX
RX
1'
2'
3'
DPX
BP1
BP2
CIR
1
2
3
f_{TX}
f_{RX}
to / from the antenna

FIG.1

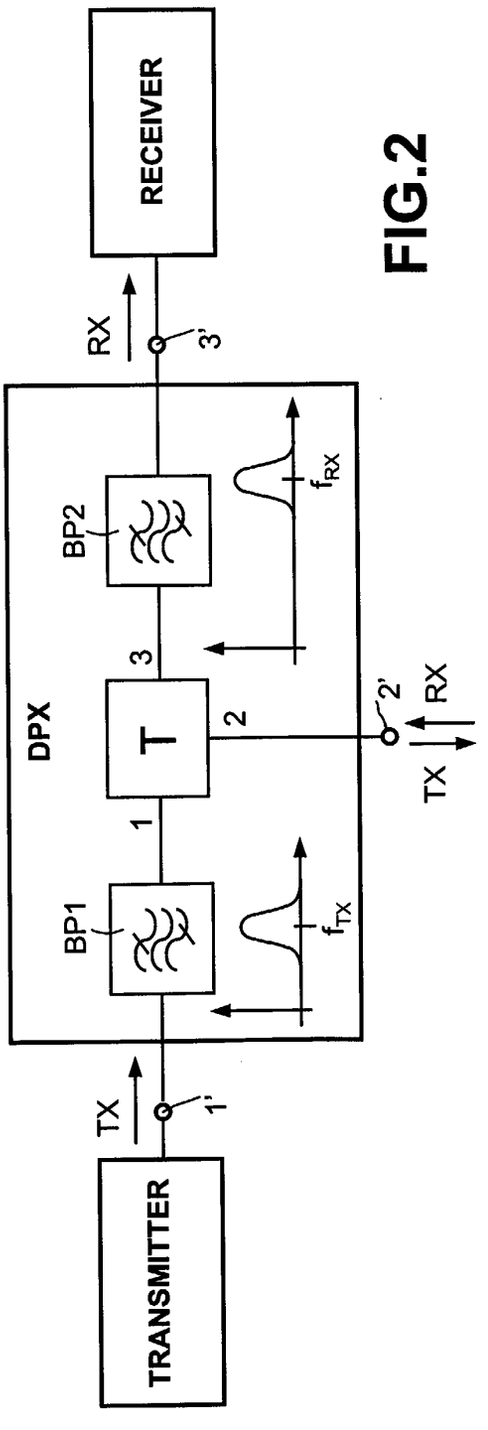
TRANSMITTER
RECEIVER
TX
RX
1'
2'
3'
DPX
BP1
BP2
T
1
2
3
f_{TX}
f_{RX}

FIG.2

FR4 MICROSTRIP TO WAVEGUIDE TRANSITION (KNOWN ART)

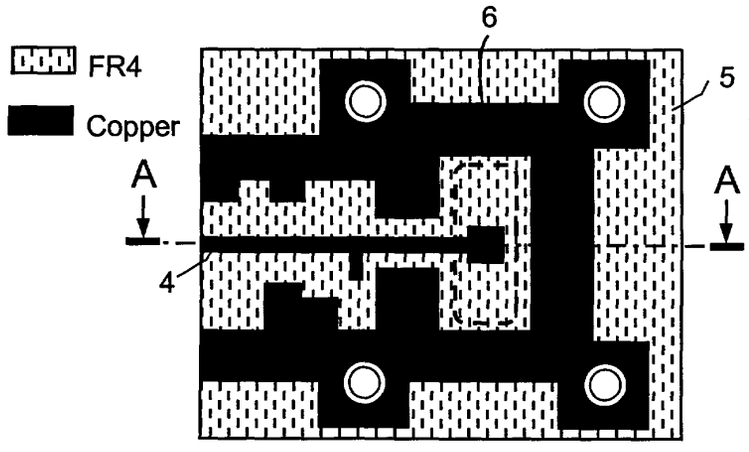

FIG. 3a (top view)

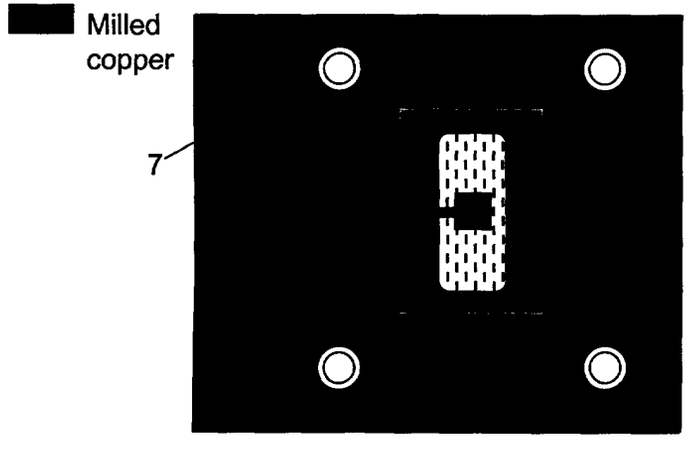

FIG. 3b (bottom view)

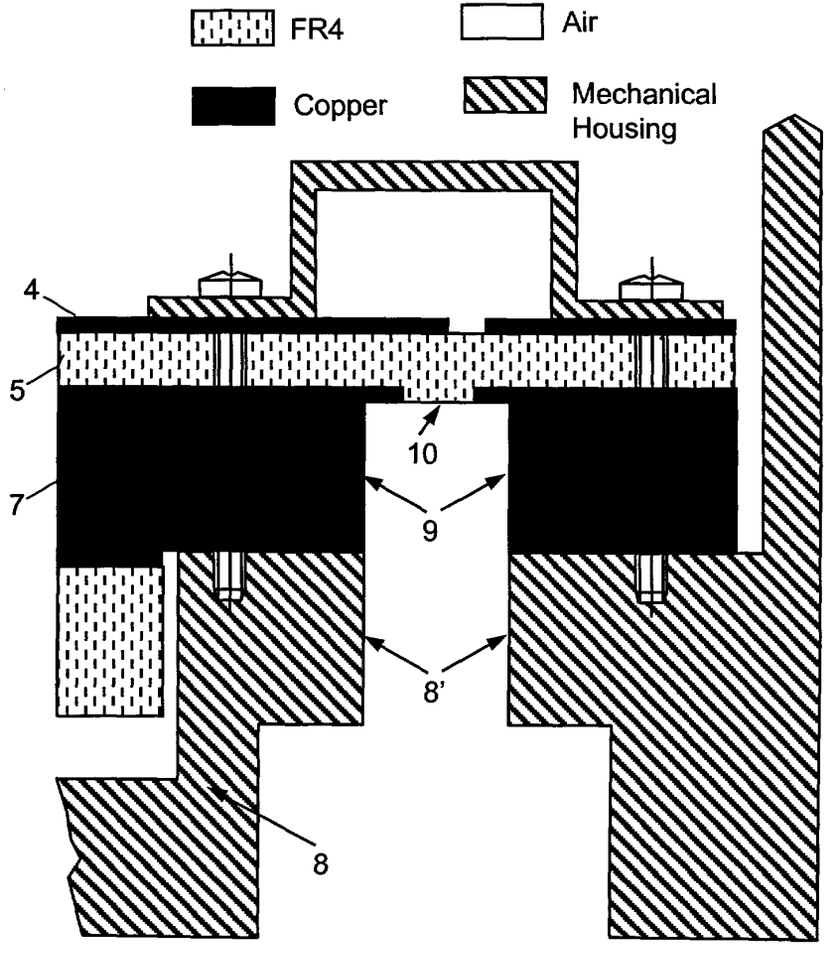

FIG. 3c - Cross-section A-A

PHOTOGRAPH OF A PLANAR FILTER OF THE KNOWN ART

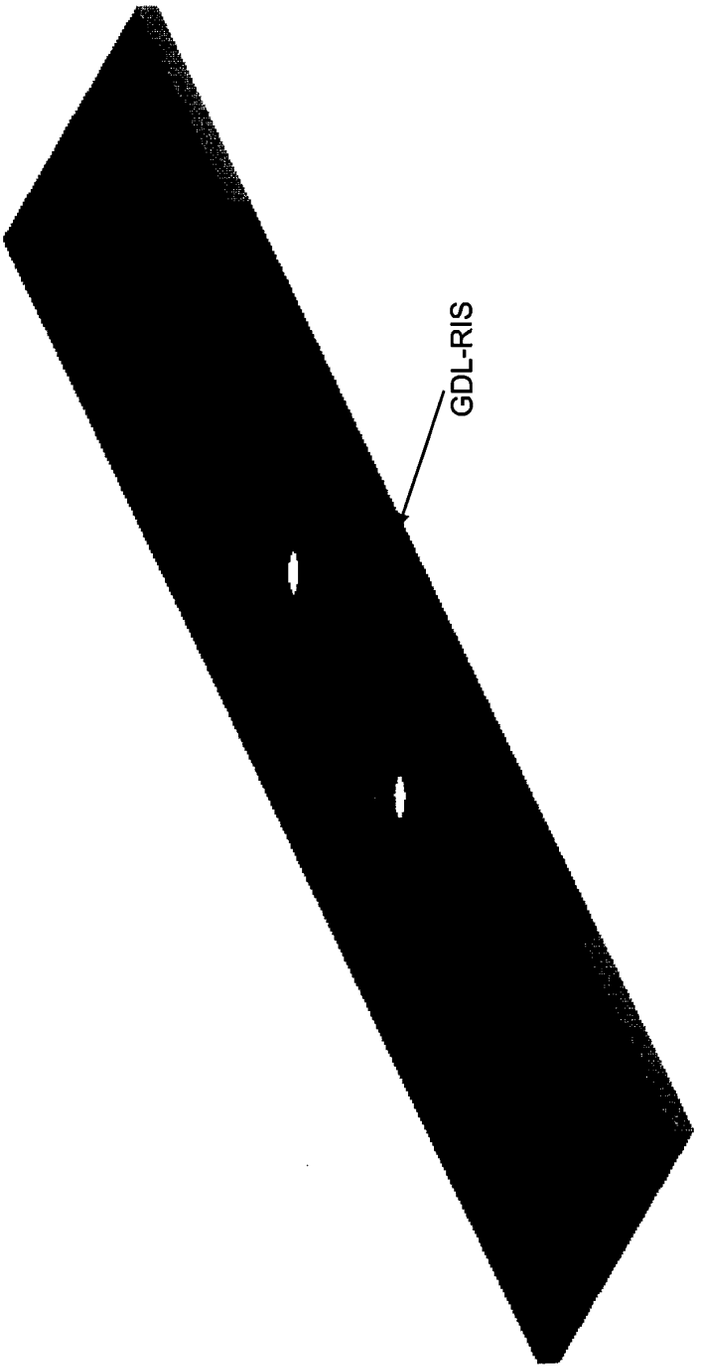

FIG.4

PHOTOGRAPHS OF THE FRONT FACE LAYOUT OF THE DUPLEXER

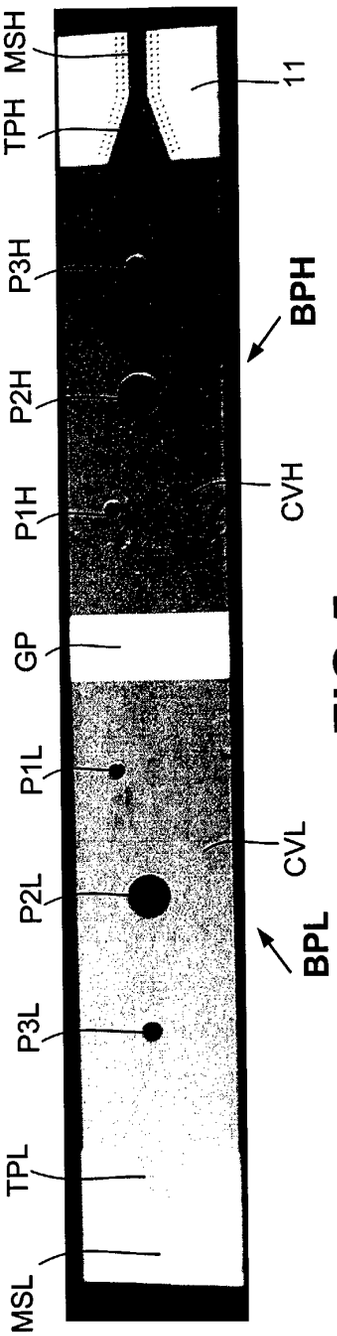

FIG.5

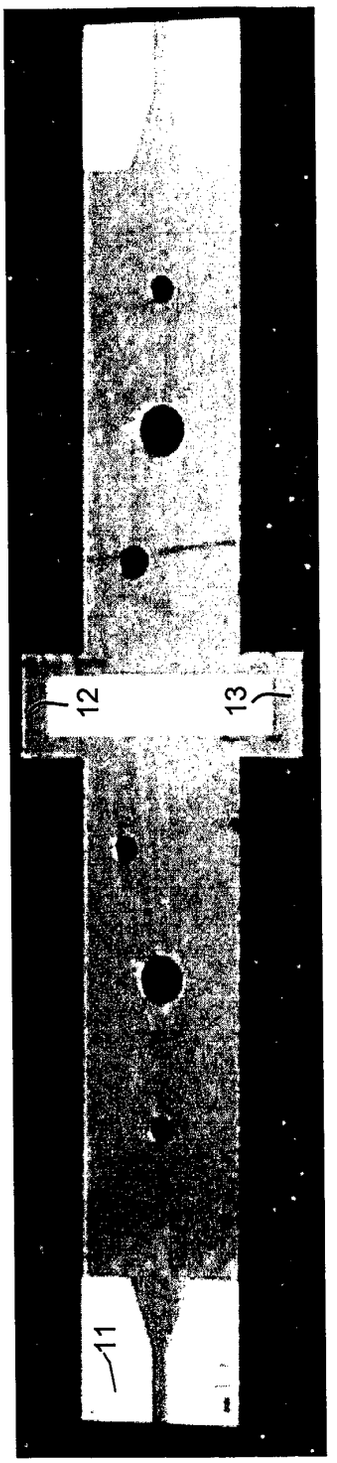

FIG.5a (preferred embodiment)

PHOTOGRAPH OF A PARTIAL MOUNTING OF THE DUPLEXER BASE

FIG.6

PHOTOGRAPH OF THE BODY OF THE TRANSITION

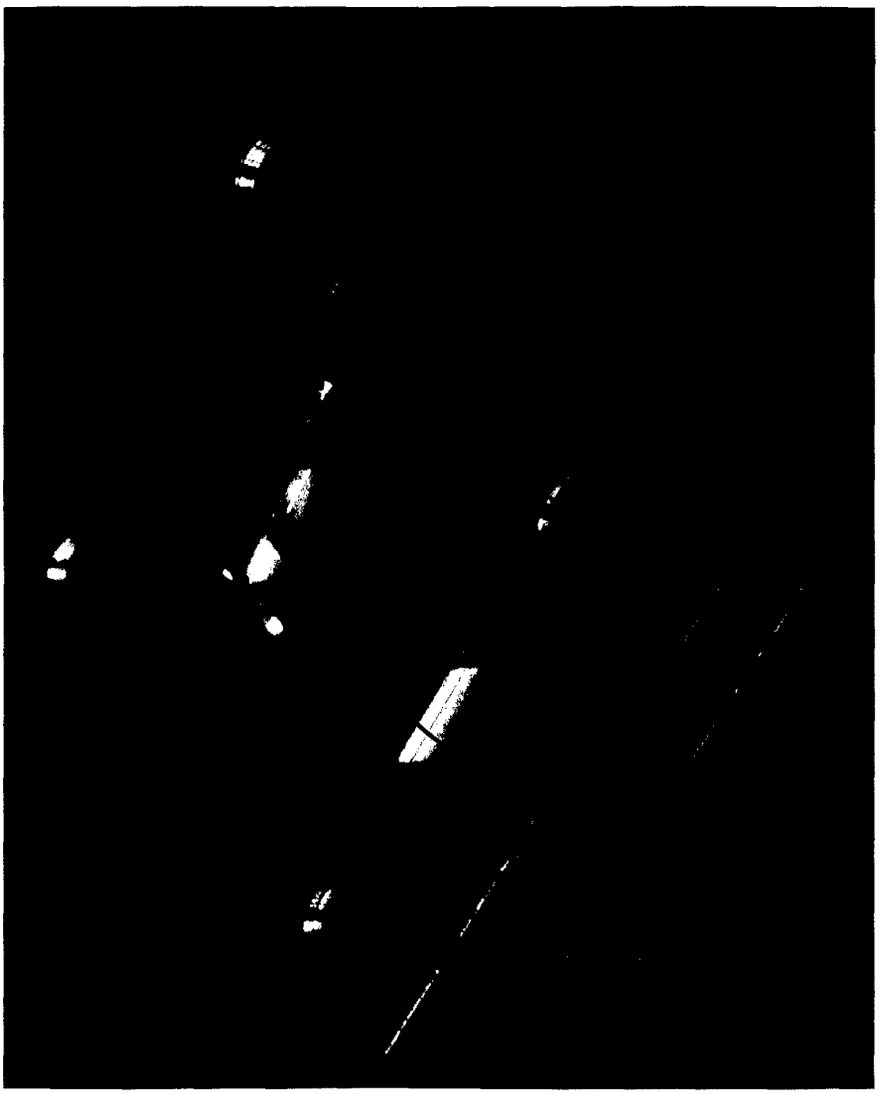

FIG.7

PHOTOGRAPH OF A PREFERRED EMBODIMENT OF THE BODY OF THE TRANSITION

FIG.8

PHOTOGRAPH OF THE DUPLEXER ASSEMBLING

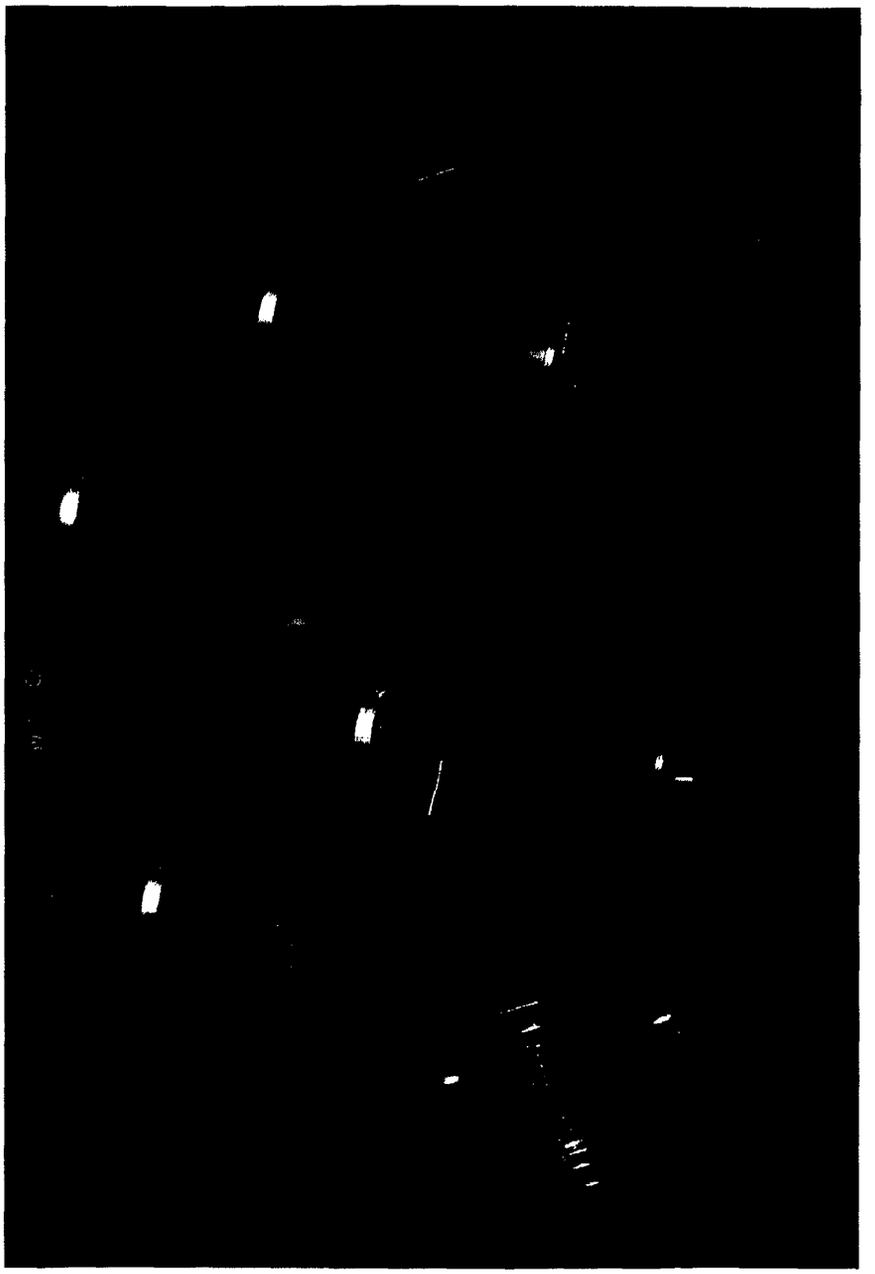

FIG.9

EXPLODED VIEW OF THE DUPLEXER FILTER

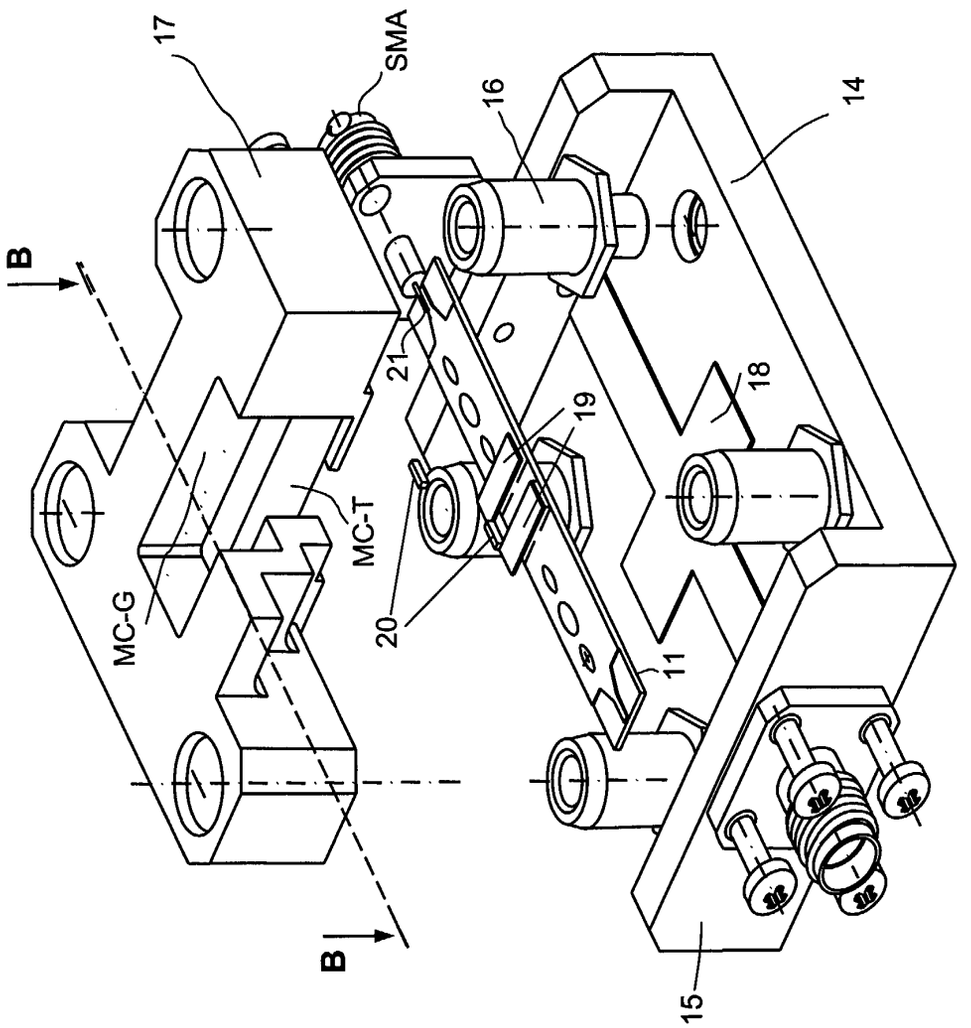

FIG.10

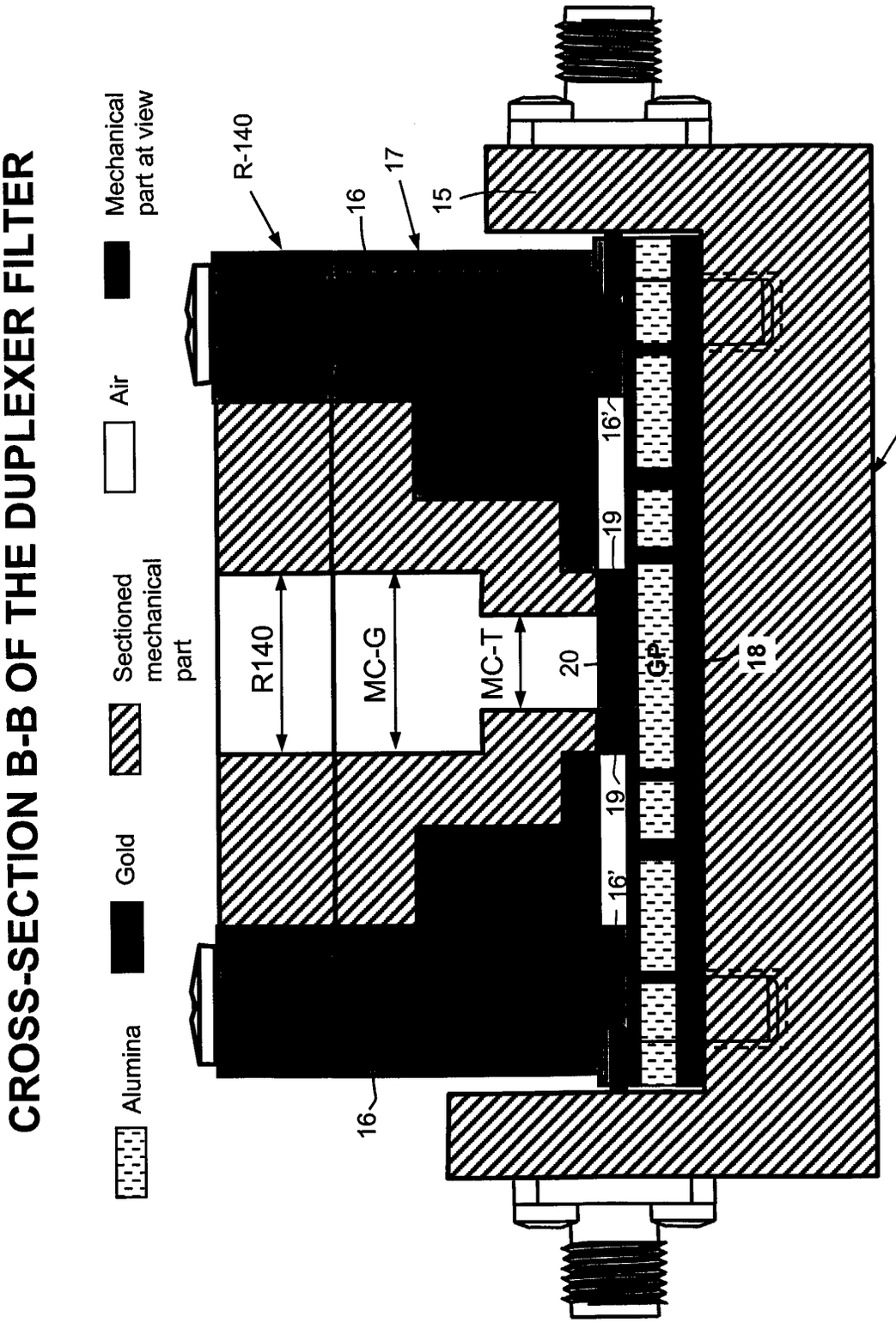
CROSS-SECTION B-B OF THE DUPLEXER FILTER
Alumina
Gold
Sectioned mechanical part
Air
Mechanical part at view
R-140
16
17
15
16'
19
R140
MC-G
MC-T
20
GP
18
14

FIG. 11

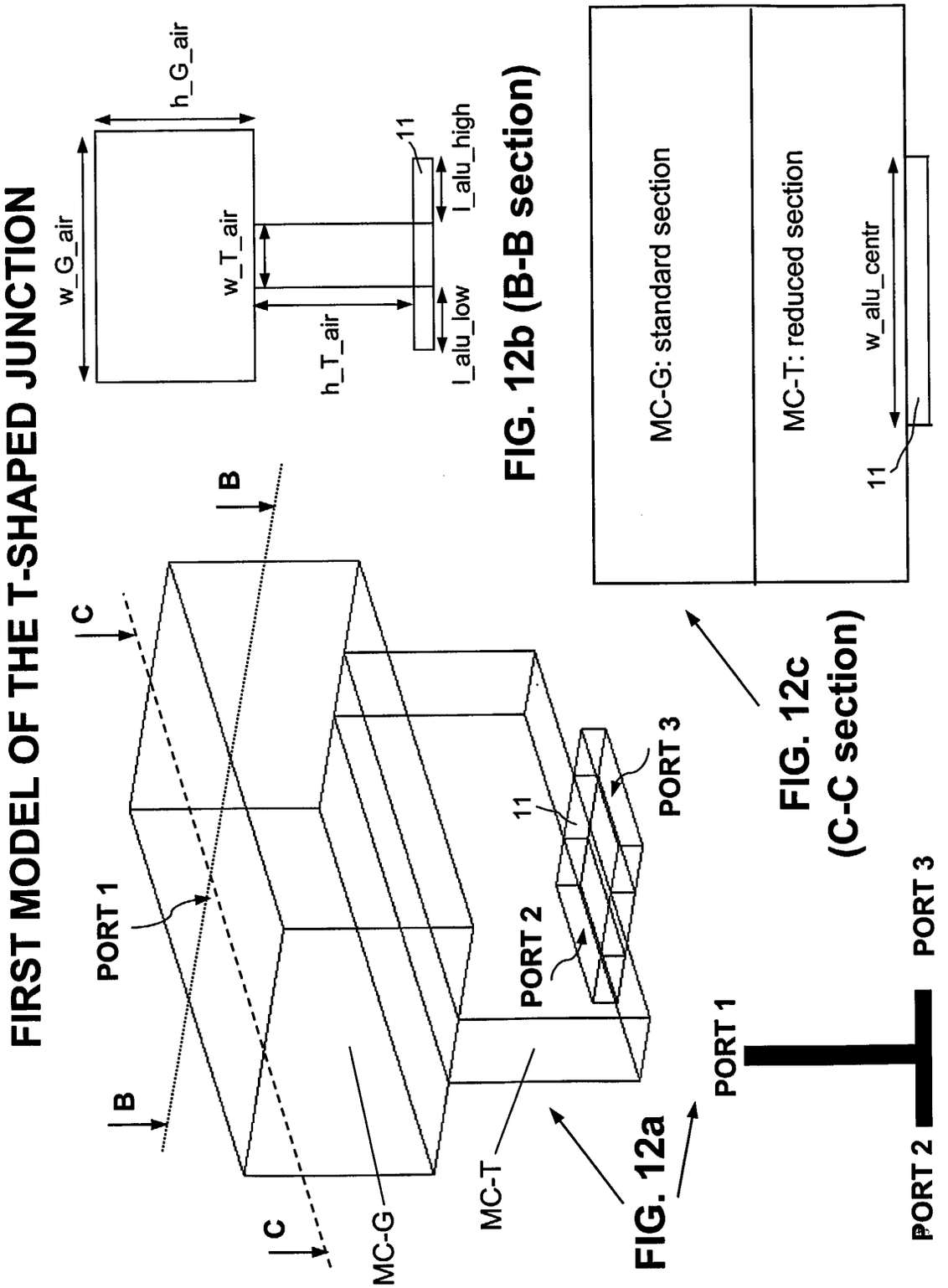
FIRST MODEL OF THE T-SHAPED JUNCTION
B
C
PORT 1
PORT 2
PORT 3
11
MC-G
MC-T
FIG. 12a
h_G_air
w_G_air
w_T_air
h_T_air
l_alu_high
l_alu_low
11
FIG. 12b (B-B section)
MC-G: standard section
MC-T: reduced section
w_alu_centr
11
FIG. 12c
(C-C section)
PORT 1
PORT 3
PORT 2

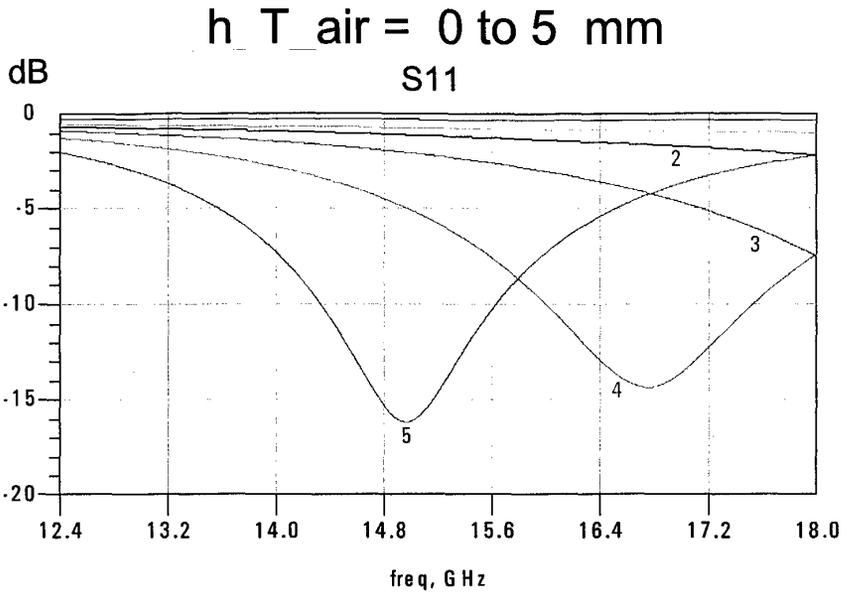

Fig.13a

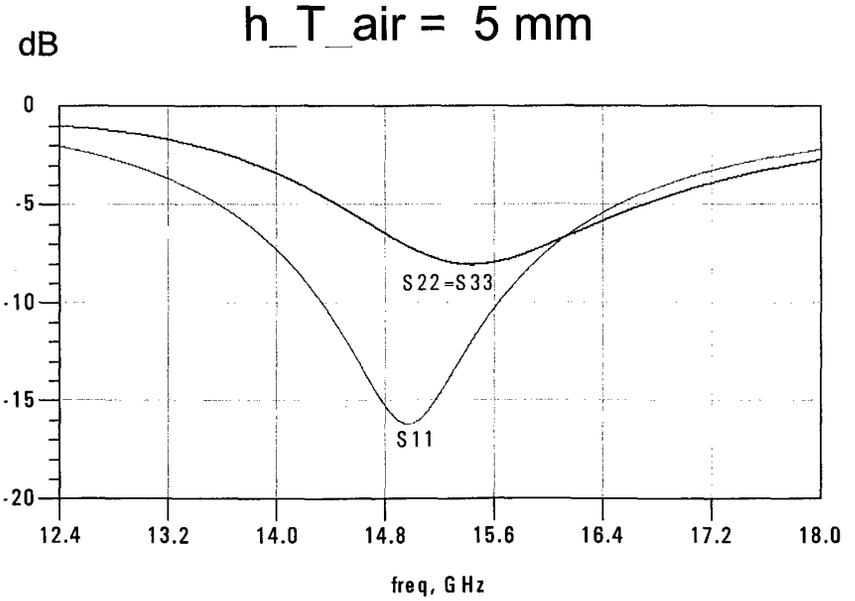

Fig.13b

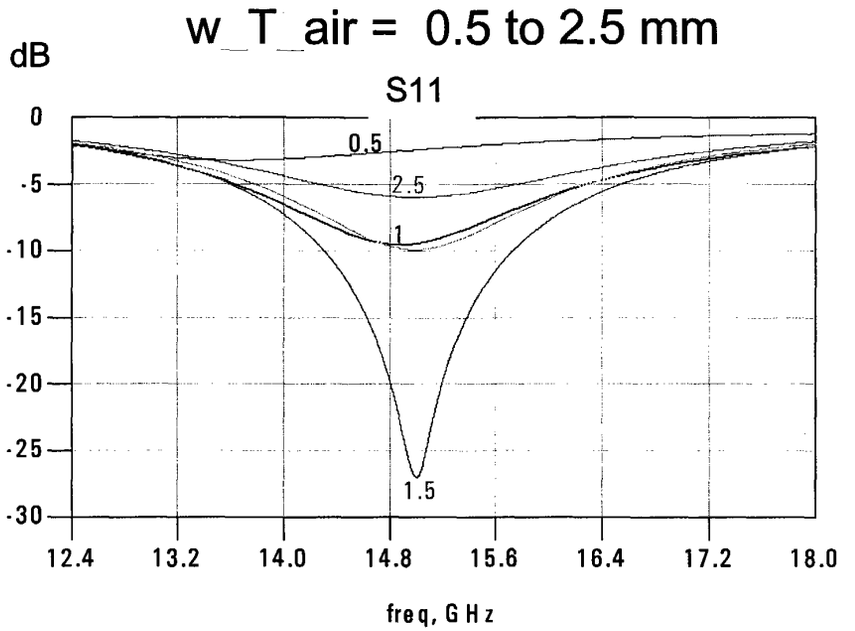

Fig.13c

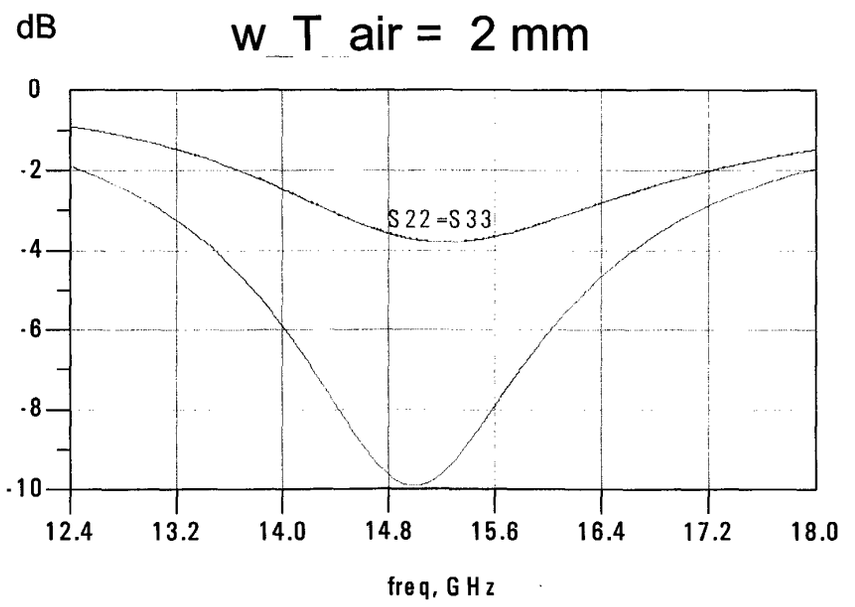

Fig.13d

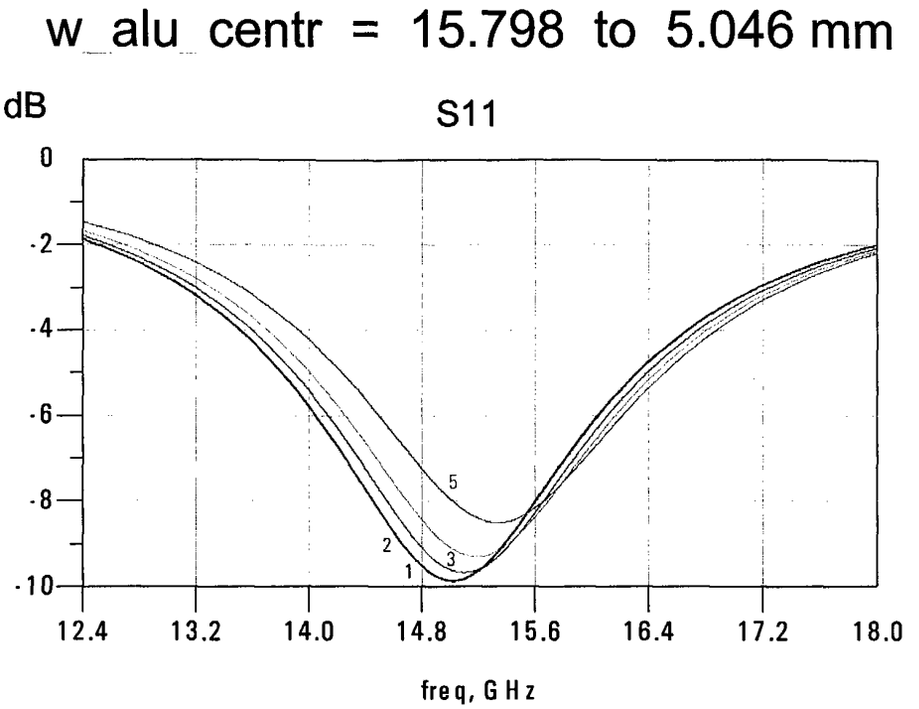

Fig.13e

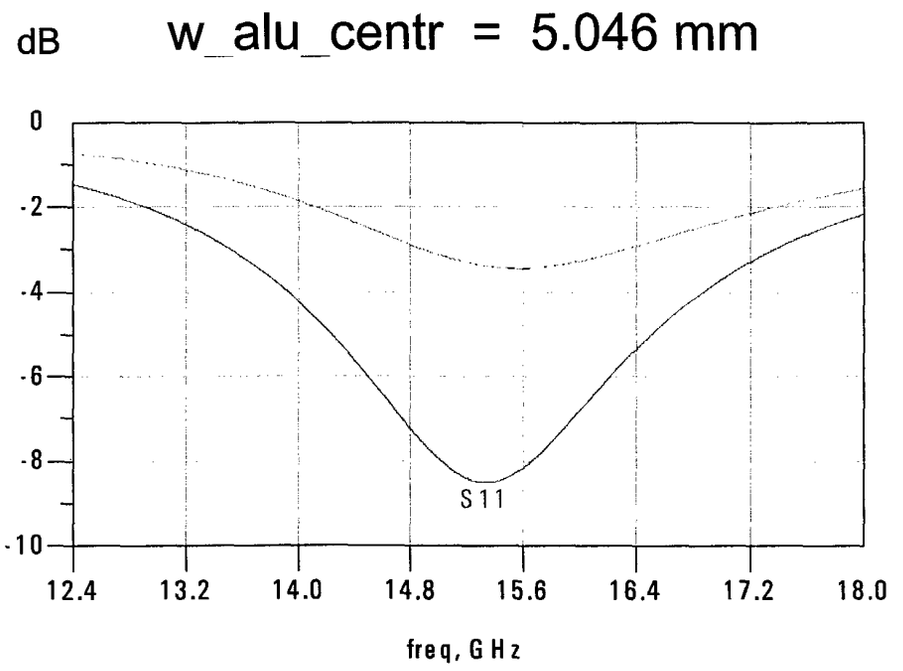

Fig.13f

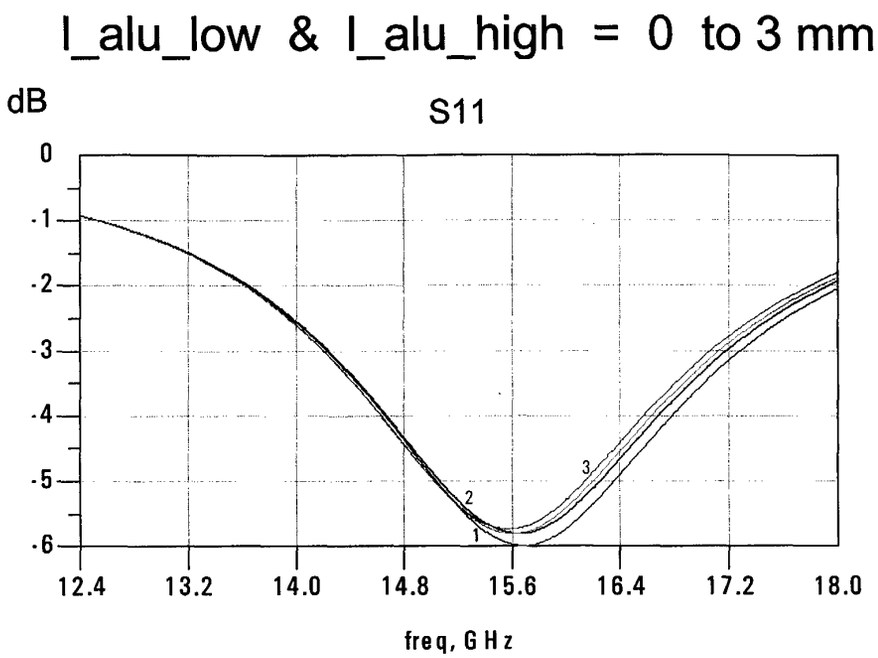

Fig.13g

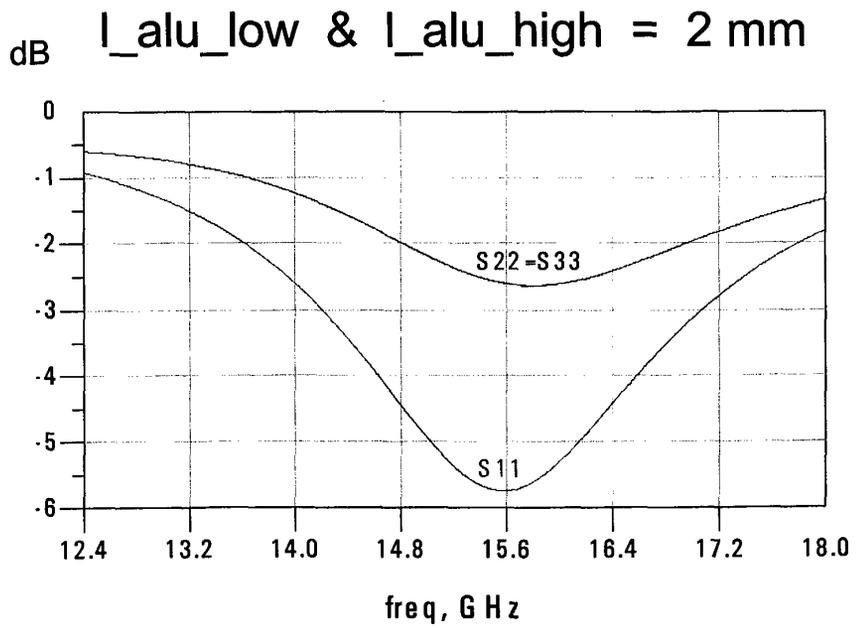

Fig.13h

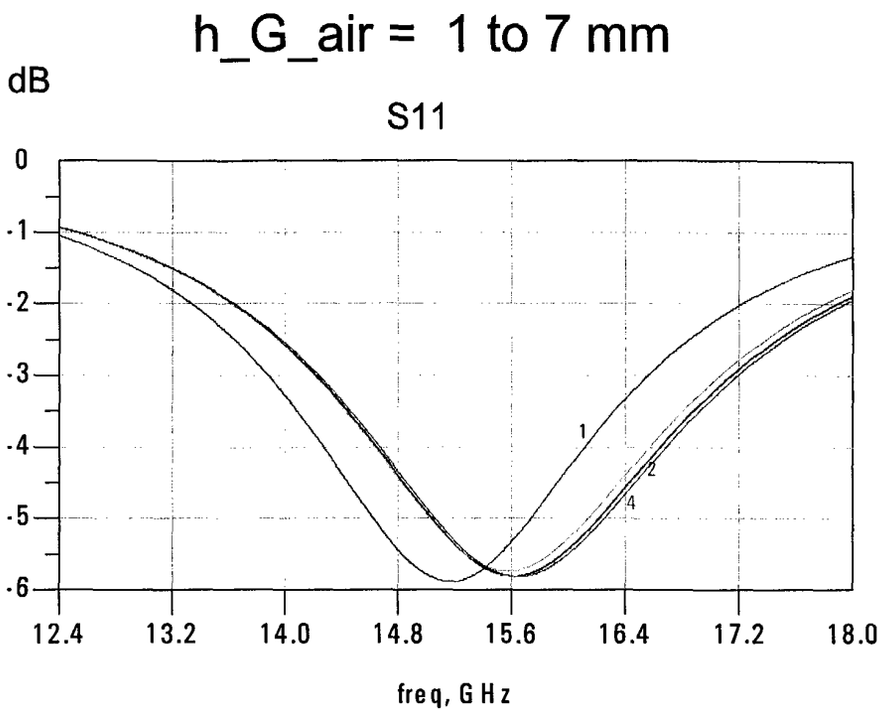

Fig.13i

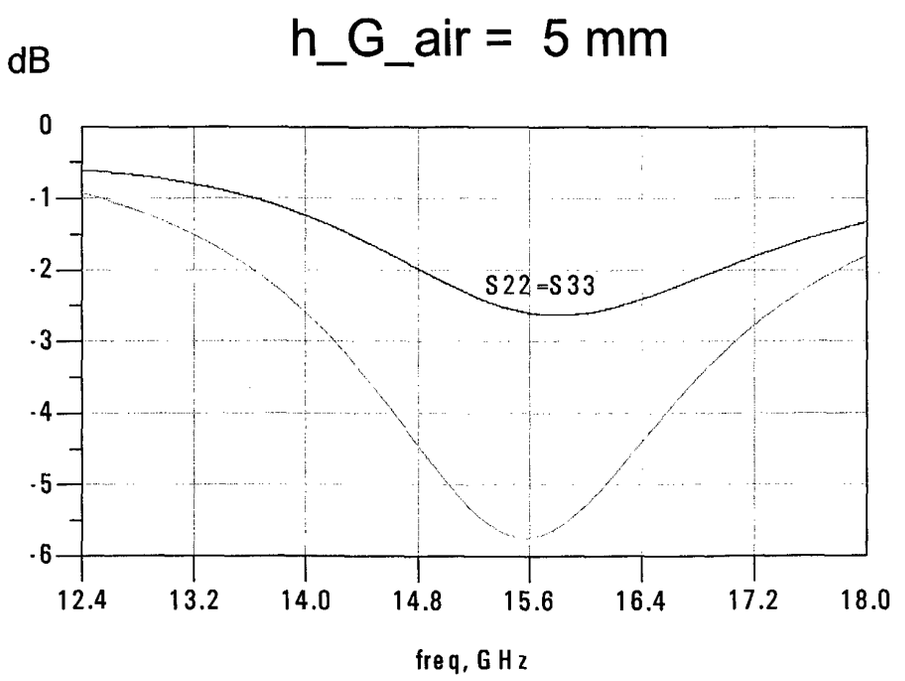

Fig.13j

Single-resonator S11 ideal filter responses

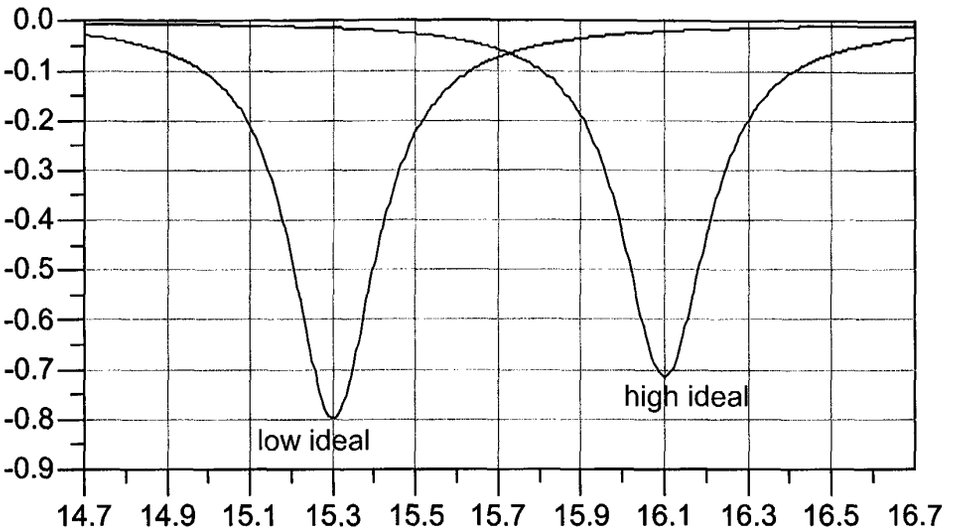

Fig.13k

Double-resonator S11 ideal filter responses

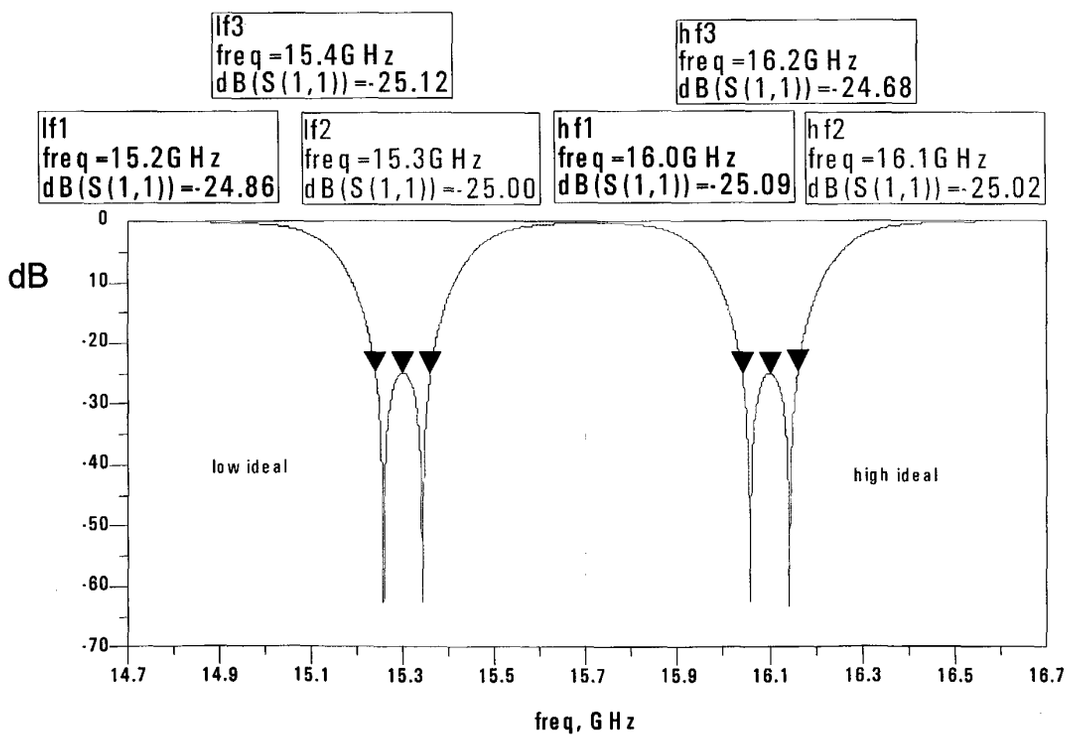

Fig.13l

MODEL OF THE TAPERED TRANSITION

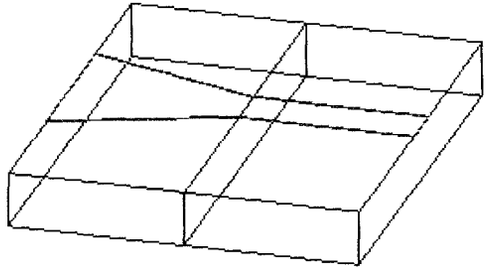

FIG. 14a

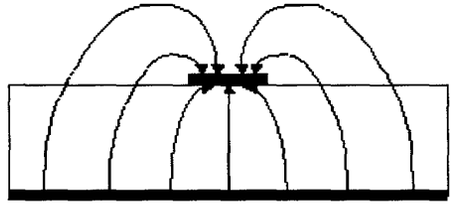

MICROSTRIP

FIG. 14b

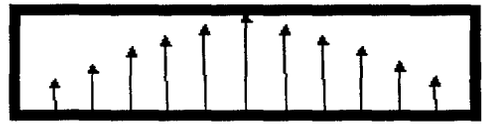

DIELECTRIC GUIDE

FIG. 14c

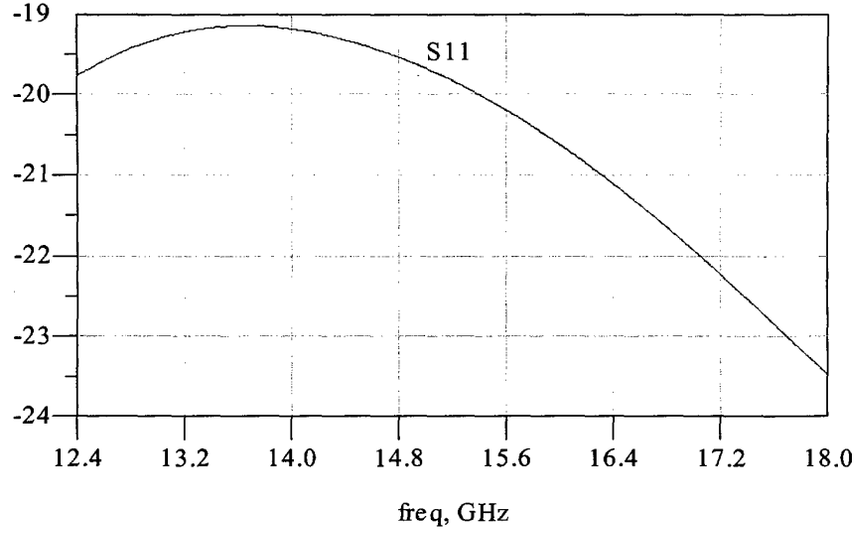

FIG. 14d

EP 1 469 548 A1

MODEL TO DESIGN FIRST RESONATORS

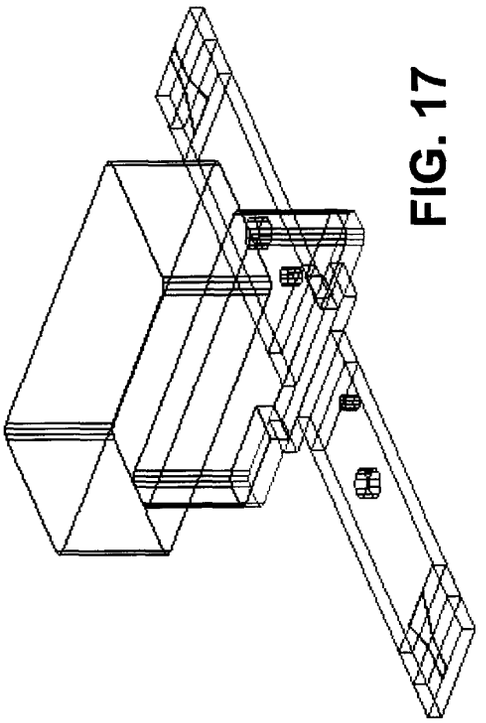

FIG. 17

MODEL TO DESIGN SECOND RESONATORS

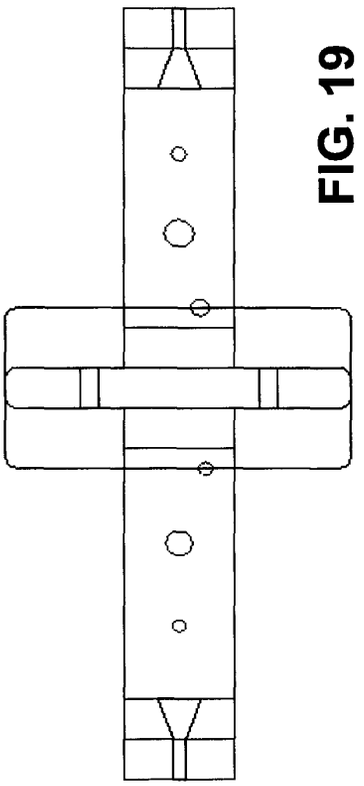

FIG. 19

SECOND MODEL OF THE T- JUNCTION

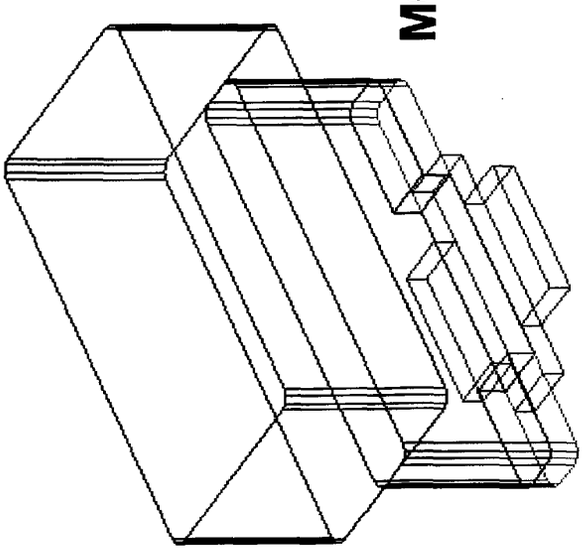

FIG. 15

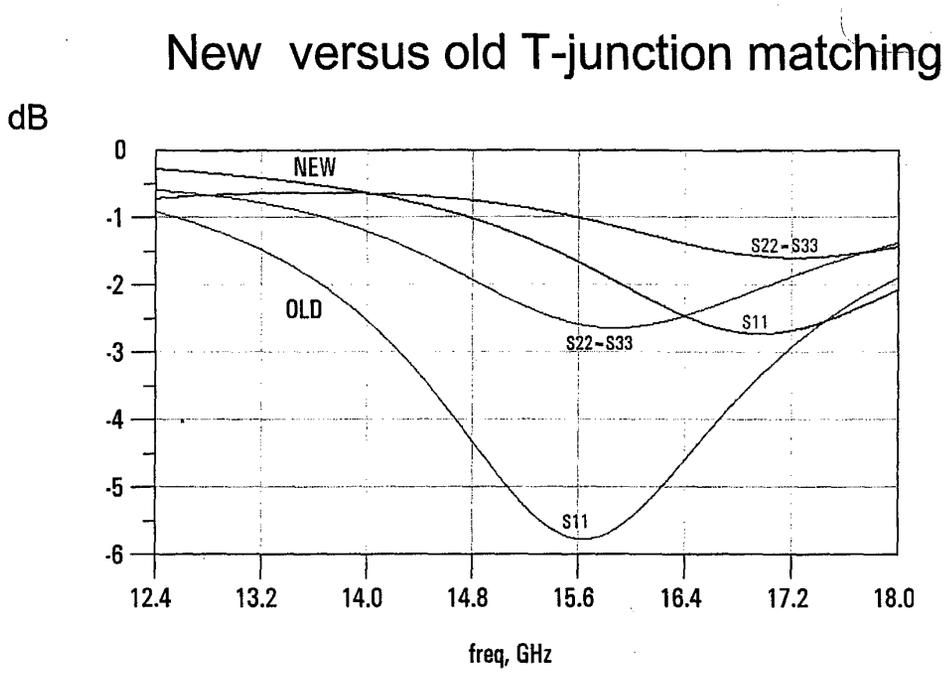

Fig.16a

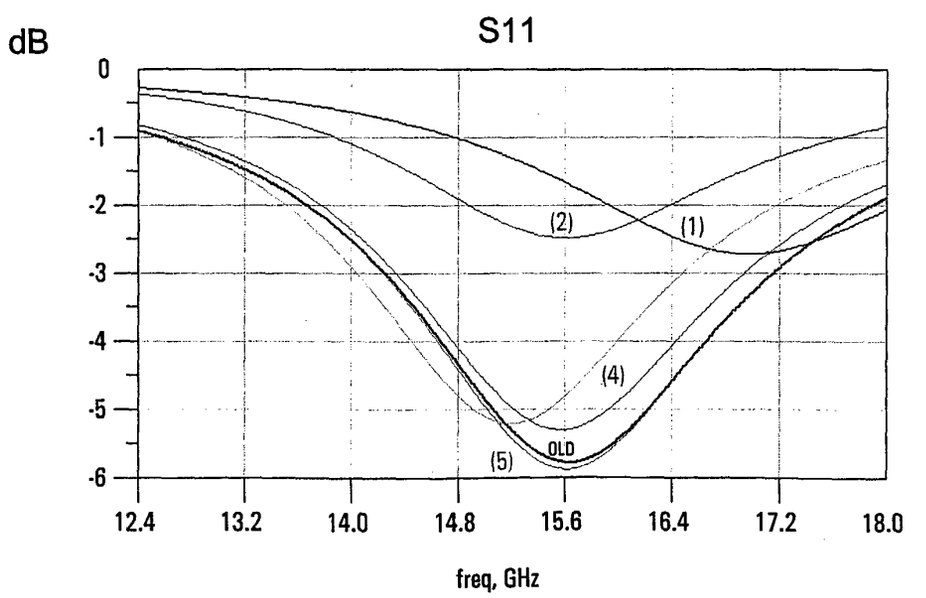

Fig.16b

Final matching of the T-junction

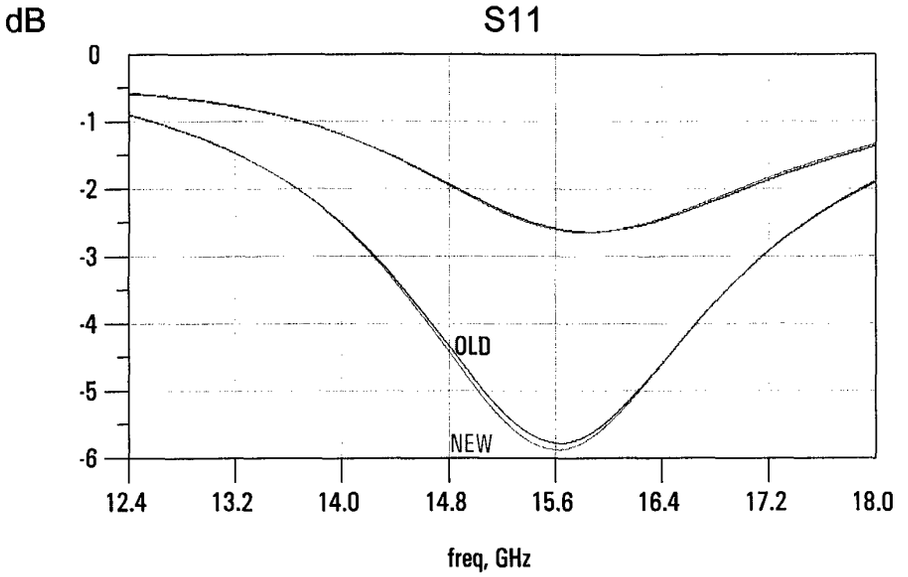

Fig.16c

Single-resonator ideal and real matching

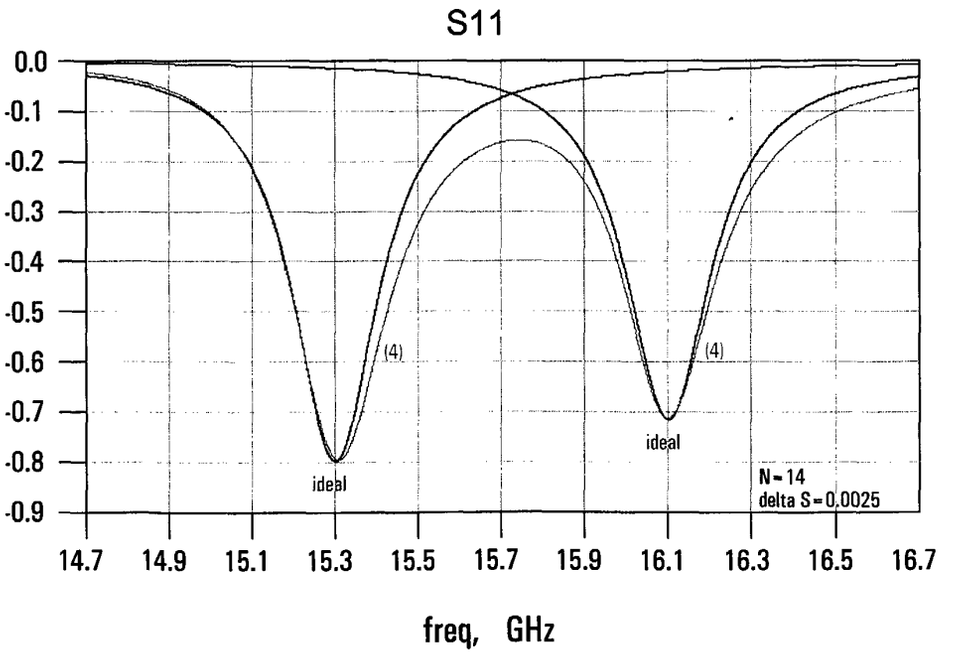

Fig.18

Double-resonator initial matching step

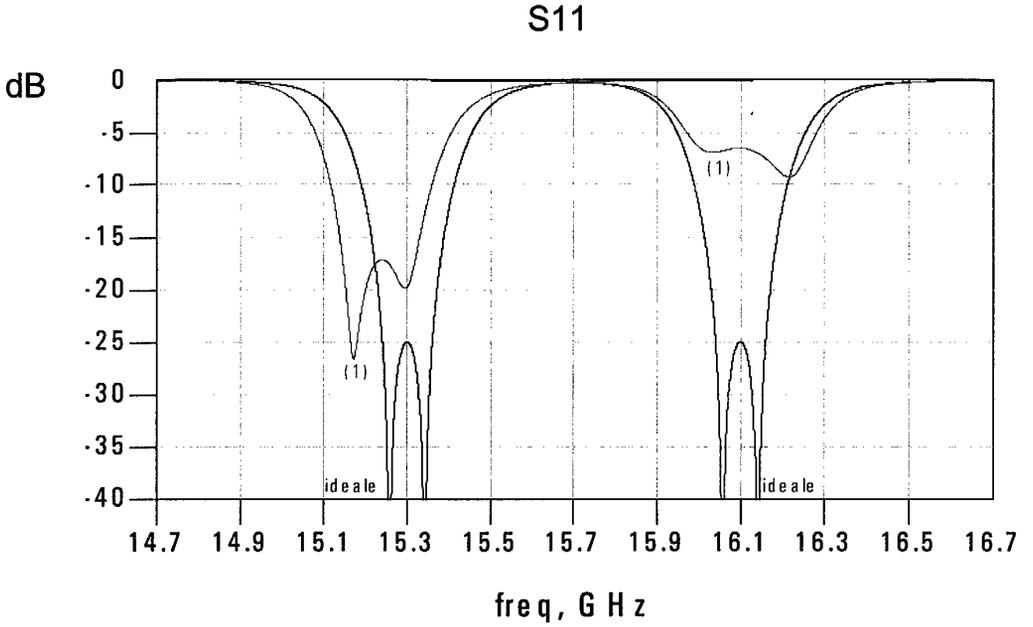

Fig.20a

Double-resonator final matching step

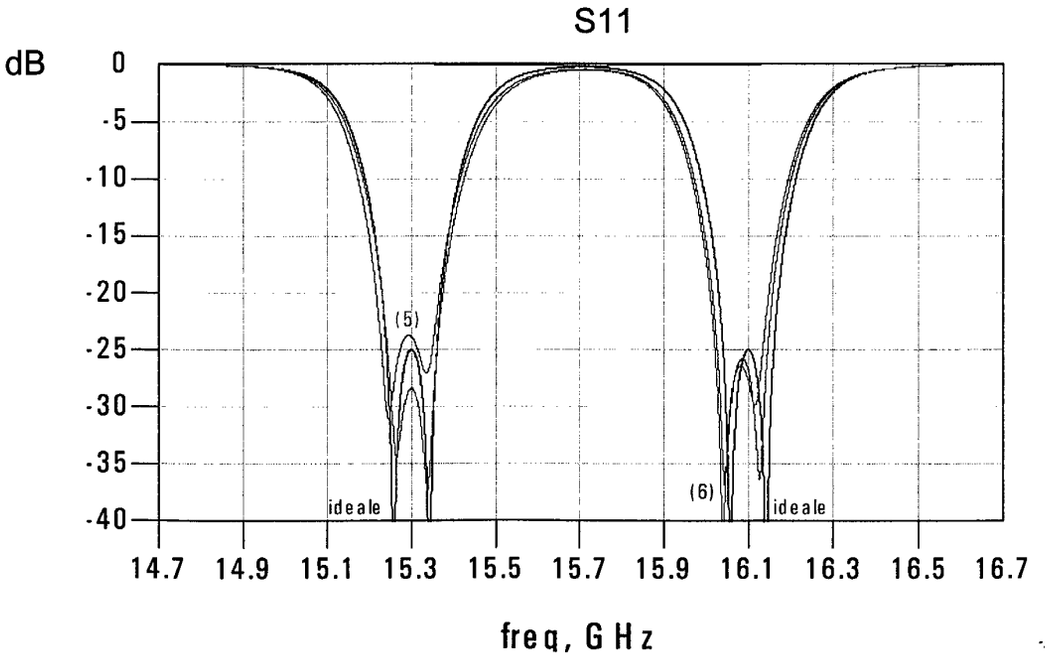

Fig.20b

TRANSMISSION AND REFLECTION CURVES OF THE DUPLEXER FILTER

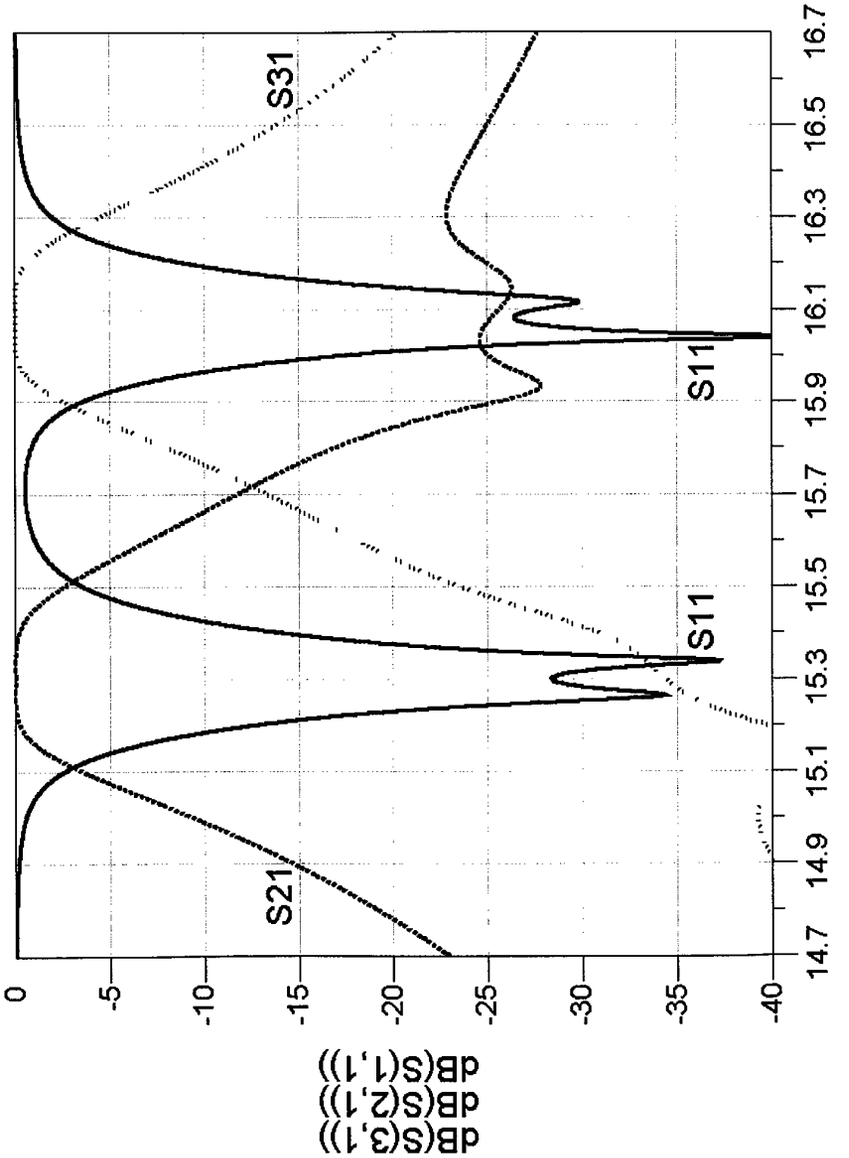

FIG.20c

European Patent Office

PARTIAL EUROPEAN SEARCH REPORT

which under Rule 45 of the European Patent Convention shall be considered, for the purposes of subsequent proceedings, as the European search report

Application Number EP 03 42 5240

DOCUMENTS CONSIDERED TO BE RELEVANT

Category	Citation of document with indication, where appropriate, of relevant passages	Relevant to claim	CLASSIFICATION OF THE APPLICATION (Int.Cl.7)
X	US 2002/027483 A1 (HIRATSUKA TOSHIRO ET AL) 7 March 2002 (2002-03-07) * paragraph [0063]; figure 10 * ---	1-13	H01P1/213
X	US 2002/097109 A1 (RAMESH MANGIPUDI ET AL) 25 July 2002 (2002-07-25) * the whole document * ---	1-13	
A	US 4 100 516 A (HALL ROGER D) 11 July 1978 (1978-07-11) * abstract; figures 1-3 * -----	1-13	

TECHNICAL FIELDS SEARCHED (Int.Cl.7)

H01P

INCOMPLETE SEARCH

The Search Division considers that the present application, or one or more of its claims, does/do not comply with the EPC to such an extent that a meaningful search into the state of the art cannot be carried out, or can only be carried out partially, for these claims.

Claims searched completely :

Claims searched incompletely :

1-13

Claims not searched :

Reason for the limitation of the search:

Severe deficiencies regarding clarity and sufficient disclosure, Articles 83 and 84 EPC

Place of search	Date of completion of the search	Examiner
MUNICH	17 September 2003	Saur, E

CATEGORY OF CITED DOCUMENTS

X : particularly relevant if taken alone
Y : particularly relevant if combined with another document of the same category
A : technological background
O : non-written disclosure
P : intermediate document

T : theory or principle underlying the invention
E : earlier patent document, but published on, or after the filing date
D : document cited in the application
L : document cited for other reasons

& : member of the same patent family, corresponding document

EPO FORM 1503 03.82 (P04C07)

ANNEX TO THE EUROPEAN SEARCH REPORT ON EUROPEAN PATENT APPLICATION NO. EP 03 42 5240

This annex lists the patent family members relating to the patent documents cited in the above-mentioned European search report. The members are as contained in the European Patent Office EDP file on
The European Patent Office is in no way liable for these particulars which are merely given for the purpose of information.

17-09-2003

Patent document cited in search report	Publication date	Patent family member(s)	Publication date
US 2002027483 A1	07-03-2002	JP 2002084101 A	22-03-2002
		DE 10143689 A1	02-05-2002
		GB 2371415 A ,B	24-07-2002
US 2002097109 A1	25-07-2002	WO 02052674 A1	04-07-2002
US 4100516 A	11-07-1978	JP 1348166 C	13-11-1986
		JP 53115161 A	07-10-1978
		JP 61011482 B	03-04-1986

EPO FORM P0459

For more details about this annex : see Official Journal of the European Patent Office, No. 12/82